

1 The macronutrient and micronutrient (iron and manganese) content 2 of icebergs

3 Jana Krause¹, Dustin Carroll², Juan Höfer^{3,4}, Jeremy Donaire^{5,6}, Eric P. Achterberg¹, Emilio Alarcón⁴, Te
4 Liu¹, Lorenz Meire^{7,8}, Kechen Zhu⁹, Mark J. Hopwood^{9*}

5 ¹ GEOMAR Helmholtz Centre for Ocean Research Kiel, Kiel, Germany

6 ² Moss Landing Marine Laboratories, San José State University, Moss Landing, California, USA

7 ³ Escuela de Ciencias del Mar, Pontificia Universidad Católica de Valparaíso, Valparaíso, Chile

8 ⁴ Centro FONDAP de Investigación en Dinámica de Ecosistemas Marinos de Altas Latitudes (IDEAL), Valdivia, Chile

9 ⁵ Facultad de Ingeniería, Universidad Andrés Bello, Viña del Mar, Chile

10 ⁶ Faculty of Sciences and Bioengineering Sciences, Vrije Universiteit Brussel, Brussels, Belgium

11 ⁷ Department of Estuarine and Delta Systems, Royal Netherlands Institute for Sea Research, Yerseke, The Netherlands

12 ⁸ Greenland Climate Research Centre, Greenland Institute of Natural Resources, Nuuk, Greenland

13 ⁹ Department of Ocean Science and Engineering, Southern University of Science and Technology, Shenzhen, China

14 *Correspondence to:* Mark J. Hopwood (Mark@sustech.edu.cn)

15 **Abstract.** Ice calved from the Antarctic and Greenland Ice Sheets or tidewater glaciers ultimately melts
16 in the ocean contributing to sea-level rise and potentially affecting marine biogeochemistry. Icebergs have
17 been described as ocean micronutrient fertilizing agents, and biological hotspots due to their potential
18 roles as platforms for marine mammals and birds. Icebergs may be especially important fertilizing agents
19 in the Southern Ocean, where **low** availability of the micronutrients iron and manganese extensively limits
20 marine primary production. Whilst icebergs have long been described as a source of iron to the ocean,
21 their nutrient load is poorly constrained and it is unclear if there are regional differences. Here we show
22 that 589 ice fragments collected from calved ice in contrasting regions spanning the Antarctic Peninsula,
23 Greenland, and smaller tidewater systems in Svalbard, Patagonia and Iceland have similar (micro)nutrient
24 concentrations with limited or no significant differences between regions. Icebergs are a minor or
25 negligible source of macronutrients to the ocean with low concentrations of NO_x^- ($\text{NO}_3^- + \text{NO}_2^-$, median
26 $0.51 \mu\text{M}$), PO_4^{3-} (median $0.04 \mu\text{M}$), and dissolved Si (dSi, median $0.02 \mu\text{M}$). In contrast, icebergs deliver
27 elevated concentrations of dissolved Fe (dFe, median 12 nM) and Mn (dMn, median 2.6 nM). Sediment
28 load for Antarctic ice (median 9 mg L^{-1} , $n=144$) was low compared to prior reported values for the Arctic
29 (up to 200 g L^{-1}). Whilst ~~T~~Total dissolvable Fe and Mn retained a strong relationship with sediment load

(both $R^2 = 0.43$, $p < 0.001$) ~~whereas~~, weaker relationships were observed for dFe ($R^2 = 0.30$, $p < 0.001$), dMn ($R^2 = 0.20$, $p < 0.001$) and dSi ($R^2 = 0.29$, $p < 0.001$). A tight correlation between total dissolvable Fe and Mn ($R^2 = 0.95$, $p < 0.001$) and a total dissolvable Mn:Fe ratio of 0.024 suggested a lithogenic origin for the majority of sediment present in ice. Dissolved Mn was ~~however~~ present at higher dMn:dFe ratios, with ~~meltwater~~ fluxes from melting ice roughly equivalent to 30% of the corresponding dFe flux. Our results ~~suggest~~ demonstrated that ~~NO_x^- and PO_4^{3-} the nutrient~~ concentrations measured in calved icebergs originate from the ice matrix ~~are consistent with an atmospheric source of NO_x^- and PO_4^{3-}~~ . Conversely, high Fe and Mn, and occasionally high dSi concentrations, are associated with englacial sediment, which experiences limited biogeochemical processing prior to release into the ocean.

1 Introduction

At the interface between ~~the arine-terminating iceeryosphere~~ and the ocean, icebergs are ~~both~~ physical and chemical agents via which ice-ocean interactions affect marine biogeochemical cycles (Enderlin et al., 2016; Helly et al., 2011; Smith Jr. et al., 2007). Icebergs are ~~often described as fertilizing agents,~~ widely characterised as a source of the micronutrient iron (Fe) to marine ecosystems ~~ecosystems~~ (Raiswell, 2011; Raiswell et al., 2008; Shaw et al., 2011), especially in ~~the context of~~ the Southern Ocean (Schwarz and Schodlok, 2009; Smith Jr. et al., 2007; Vernet et al., 2011). Iron availability is a major factor limiting primary production in the Southern Ocean (Martin et al., 1990a, b; Moore et al., 2013) and thus regional changes in Fe supply can have pronounced ecosystem effects (Schwarz and Schodlok, 2009; Wu and Hou, 2017). Whilst icebergs are recognised as a potentially climatically sensitive Fe source (IPCC, 2019), the importance of their role for delivery of other micro- and macro-nutrients remains to be quantified. However, the fertilizing effect of icebergs is likely regionally dependent due to changes in the identity of the (micro)nutrients limiting marine primary production, and perhaps also due to regional changes in the nutrient load of icebergs. In the Southern Ocean, iron (Fe) is thought to be the main nutrient limiting phytoplankton growth throughout much of the growth season and so changes to regional Fe supply can have ecosystem effects (Martin et al., 1990a, b; Moore et al., 2013). A critical research challenge is therefore to ~~constrain Fe sources and sinks in the Southern Ocean and to assess their climatic~~

57 ~~sensitivity (Martin, 1990; Wadley et al., 2014). Icebergs are one such Fe source to pelagic ecosystems~~
58 ~~(Raiswell, 2011; Raiswell et al., 2008; Shaw et al., 2011). Icebergs have long been described as an~~
59 ~~important Fe source via delivery of both englacial sediment and the dissolved components of ice melt~~
60 ~~(Hart, 1934; Lin et al., 2011; Raiswell et al., 2008). Positive chlorophyll anomalies following iceberg~~
61 ~~passage in the Southern Ocean during the growth season have been detected by satellite derived~~
62 ~~chlorophyll measurements and these are usually attributed to Fe fertilization (Schwarz and Schodlok,~~
63 ~~2009; Wu and Hou, 2017). However, Fe may not be the only micronutrient to limit marine primary~~
64 ~~production around Antarctica. Recent work has, for example, suggested that low dissolved manganese~~
65 (Mn) concentrations are a further co-limiting factor for phytoplankton growth in parts of the Southern
66 Ocean (Browning et al., 2021; Hawco et al., 2022; Latour et al., 2021). As Fe and Mn share similar
67 sources, icebergs might also be an equally important source term for the polar marine Mn cycle (Forsch
68 et al., 2021).

69
70 In contrast to Antarctica, Fe-limitation of marine phytoplankton growth in the Arctic is a less prominent
71 feature. ~~Fe limitation is sparsely reported in the Arctic (Taylor et al., 2013) and~~ largely confined to
72 offshore areas of the high-latitude North Atlantic away from typical iceberg trajectories (Nielsdottir et al.,
73 2009; Ryan-Keogh et al., 2013). Phytoplankton growth within regions around Greenland affected by
74 icebergs is more often limited by nitrate availability (Randelhoff et al., 2020, Krisch et al., 2020). With
75 icebergs thought to supply only limited concentrations of nitrate and phosphate to the ocean, a direct
76 iceberg fertilization effect is not expected in nitrate-limited marine regions (Shulenberger, 1983).
77 ~~However, The macronutrient content of icebergs is however poorly constrained, especially for components~~
78 ~~other than Fe. Although subject to large uncertainties,~~ icebergs could be a modest source of silica to the
79 marine environment (Hawkings et al., 2017; Meire et al., 2016) which might have ecological effects.
80 ~~Whilst high macronutrient concentrations are found throughout the Southern Ocean, D~~ dissolved silica
81 (dSi) availability often limits diatom growth in the Arctic due to its depletion prior to nitrate (Krause et
82 al., 2018, 2019).

84 In order to understand how iceberg-derived fluxes of (micro)nutrients may change regionally with climate
85 change and glacier retreat inland, it is necessary to understand the origin and fate of nutrients within
86 calved icebergs at sea. The nutrient load of icebergs can be broadly separated into processes which affect
87 the nutrient concentration of the ice matrix (Fischer et al., 2015; Hansson, 1994), and processes associated
88 with sediment incorporation (Alley et al., 1997; Knight, 1997; Mugford and Dowdeswell, 2010). Internal
89 cycling may also critically redistribute (micro)nutrients and affect the relative abundance of elements in
90 both dissolved (<0.2 µm) and particulate (>0.2 µm) phases. The ultimate origin of nutrients in icebergs
91 could be argued to be atmospheric (Fischer et al., 2015; Hansson, 1994). Inland precipitation and aerosol
92 deposition on ice surfaces will exert a large influence on the nutrient content of bulk ice which is
93 ultimately calved into the ocean as icebergs (Vernet et al., 2011). However, processes beyond the ice-
94 atmosphere interface may also affect the nutrient content of ice. Furthermore, internal cycling may also
95 critically redistribute (micro)nutrients and affect the relative abundance of elements in both dissolved
96 (<0.2 µm) and particulate (>0.2 µm) phases. Landslides onto ice surfaces, and the movement of basal ice
97 over bedrock or subglacial sediments create layers of ice visibly enriched in sediment (Alley et al., 1997;
98 Knight, 1997; Mugford and Dowdeswell, 2010). Some fraction of the labile phases in englacial these
99 sediments; particularly for the elements Fe, Mn and silica, which are present at high abundances; may
100 ultimately be transformed into bioaccessible nutrients in the ocean (Forsch et al., 2021; Hawkings et al.,
101 2017; Raiswell, 2011). How sediment is gained and lost from ice before, during and after iceberg calving
102 ~~therefore~~ might therefore exert some influence on measured (micro)nutrient concentrations in melting
103 icebergs at sea (Hopwood et al., 2019).

104
105 On exposed ice surfaces during the growth season, cryoconite formation and the growth of algae are
106 notable features which will act to re-distribute nutrients between inorganic and organic pools and to
107 amplify heterogeneity in the distribution of nutrients within ice (Cook et al., 2015; Rozwalak et al., 2022;
108 Stibal et al., 2017). These processes ~~will~~ occur alongside, and likely interact with, other photochemical
109 reactions (Kim et al., 2010; Kim et al., 2024). Whilst iceberg calving may temporarily disturb features
110 present on ice surfaces, and the rolling of smaller icebergs will regularly interrupt cryoconite growth on
111 calved ice surfaces, long-lived icebergs may continue to accumulate the effects of photochemical

112 processes and re-develop cryoconite. The nutrient content of icebergs, nutrient distributions and their
113 ratios might therefore not be static and in fact subject to semi-continuous changes.

114
115 As ice moves downstream from ice sheets to the coastline, critical physical processes may exert a strong
116 influence on the characteristics of the ice which ultimately calves into the ocean (Smith et al., 2019). At
117 the base of floating ice tongues and ice shelves, the melt-rates of basal ice layers exposed to warm ocean
118 waters can be rapid. Beneath the floating ice tongue of Nioghalvfjærdsbræ in northeast Greenland, for
119 example, a melt rate of $8.6 \pm 1.4 \text{ m year}^{-1}$ is likely sufficient to remove most sediment-rich basal ice prior
120 to iceberg calving (Huhn et al., 2021). In other similar cases worldwide, calved ice may ultimately be
121 deprived of basal layers which might otherwise have carried distinct labile sediment loadings reflecting
122 subglacial processes (Smith et al., 2019). Nevertheless, post-calving the nutrient content of ice may still
123 be strongly affected by ‘new’ ice-sediment interactions. Icebergs which become grounded, or scour
124 shallow coastal sediments, may temporarily re-acquire a basal layer loaded with sediment (Gutt et al.,
125 1996; Syvitski et al., 1987; Woodworth-Lynas et al., 1991). Scoured sediments may be physically and
126 chemically distinct from those acquired from land-slides or basal glacial processes and thus also
127 temporarily introduce different nutrient ratios and concentrations in ice and melt water (Forsch et al.,
128 2021).

129
130 Finally, whilst many research questions concerning the effects of the cryosphere on the ocean relate to
131 melting processes, marine ice formation is a mechanism via which ice growth can occur in the water
132 column (Craven et al., 2009; Lewis and Perkin, 1986; Oerter et al., 1992). Marine ice is formed from
133 supercooled seawater around Antarctica via the formation of platelet, or frazil, ice crystals. Whilst the
134 chemical composition of this ice is poorly studied, measurements from the Amery Ice Shelf suggest
135 marine ice has relatively high dissolved Fe (dFe) concentrations (e.g. 339-691 nM dFe, Herraiz-
136 Borreguero et al., 2016). The origin of this dFe may be subglacial, potentially indicating a synergistic
137 effect between subglacial and ice melt Fe sources. Similar synergistic effects have been suggested from
138 model studies concerning sea ice and ice shelves, whereby sea ice may trap and later release Fe that
139 originates from ice shelves (Person et al., 2021). A ‘source-to-sink’ narrative concerning iceberg-derived

140 (micro)nutrient delivery from ice directly into the ocean may therefore be over-simplistic. It is important
141 to recognise that the extent of spatial and temporal overlap between different (micro)nutrient sources may
142 result in interactive effects in annual budgets. Such effects could arise due to the underlying physical
143 processes and/or the seasonal timing of micro(nutrient) sources and sinks (Boyd et al., 2012; Person et
144 al., 2021).

145
146 ~~The (micro)nutrient content of icebergs and the associated fluxes of (micro)nutrients to the marine~~
147 ~~environment have been commented on around Greenland, Antarctica, and in smaller catchments around~~
148 ~~Svalbard (Cantoni et al., 2020; Nomura et al., 2023; Smith Jr. et al., 2007). Icebergs are widely thought~~
149 ~~to constitute a major source of Fe, particularly particulate Fe, to the ocean (Lin et al., 2011; Lin and~~
150 ~~Twining, 2012; Raiswell et al., 2016). We hypothesize that dMn, which shares similar sources with dFe,~~
151 ~~but is less susceptible to scavenging in the ocean, may also be delivered by icebergs with comparable~~
152 ~~annual fluxes to dFe. Several studies have also hinted at considerable dSi (up to 10 μM , Meire et al.,~~
153 ~~2016) or bioaccessible nitrogen concentrations (up to 5 μM) within ice (Parker et al., 1978; Vernet et al.,~~
154 ~~2011). Macronutrient concentrations in glacial ice are primarily hypothesized to reflect atmospheric~~
155 ~~deposition (Vernet et al., 2011), but it is unclear whether or not concentrations in calved ice largely reflect~~
156 ~~those originally deposited on ice sheet surfaces. The extent to which sediment incorporation into ice~~
157 ~~affects nutrient dynamics in ice melt also remains unclear. Are macronutrient and micronutrient~~
158 ~~concentrations in ice comparable at regional scales, or are there important regional differences due to~~
159 ~~changes in basal ice layer thickness, sediment load, and sediment acquisition/loss processes in nearshore~~
160 ~~waters between regions? Calved ice from small marine terminating glaciers in Svalbard, for example, can~~
161 ~~have extremely high sediment loads of up to 200 g L^{-1} (Dowdeswell and Dowdeswell, 1989), compared~~
162 ~~to lower values of 0.6–1.2 g L^{-1} in the Weddell Sea (Shaw et al., 2011). Are higher sediment loads also~~
163 ~~accompanied by increased concentrations of dissolved silica and trace metals in ice melt? Or,~~
164 ~~alternatively, is the loss of sediment from ice too fast, and any associated chemical weathering processes~~
165 ~~too slow, to significantly affect the composition of ice melt?~~

Commented [A1]: Cut/trim

167 In order to evaluate whether or not there are regional differences in the (micro)nutrient content of icebergs
168 and the associated fluxes into the ocean, here we assess the concentration of macronutrients (NO_x^- , dSi
169 and PO_4^{3-}), micronutrients (dissolved Fe and Mn) and total dissolvable metals (Fe and Mn) from calved
170 ice across multiple Arctic and Antarctic catchments. In order to investigate potential spatial and temporal
171 biases associated with seasonal shifts and the general targeting of smaller ice fragments to collect samples,
172 we include repeat samples from five campaigns in Nuup Kangerlua (a fjord hosting three marine-
173 terminating glaciers in southwest Greenland) and a comparison of recently calved ice from inshore and
174 offshore ice samples in Disko Bay (west Greenland). Throughout, we test the null hypothesis that icebergs
175 from different regions have no differences in macronutrient or micronutrient (Fe and Mn) concentrations.

176 **2 Methods**

177 **2.1 Sample collection**

178 Iceberg samples were collected by hand or by using nylon nets to snag ice floating fragments. Sample
179 collection was randomized at each field site location (Fig. 1 and Supp. Table 1) by collecting ice samples
180 at regular intervals along pre-defined transects. 1–5 kg ice pieces were retained in low-density
181 polyethylene (LDPE) bags and melted at room temperature. The first 3 aliquots of meltwater were
182 discarded to rinse the LDPE bags. Meltwater was then syringe filtered (0.2 μm , polyvinyl difluoride,
183 Millipore) into pre-cleaned 125 mL LDPE bottles for dissolved trace metal analysis and 20 mL
184 polypropylene tubes for dissolved nutrient analysis. All plasticware for trace metal sample collection was
185 pre-cleaned using a three-stage protocol: detergent, 1 week soak in HCl (1 M reagent grade), and 1 week
186 soak in HNO_3 (1 M reagent grade) with three deionized water rinses after each stage. Filters for trace
187 metal analysis were pre-rinsed with HCl (1 M reagent grade) followed by deionized water. Some
188 unfiltered samples were also retained for total dissolvable metal analysis.

189
190 In Disko Bay (west Greenland), a targeted exercise was conducted to test whether distinct regional
191 patterns of ice nutrient concentrations could be associated with specific calving locations. During cruise
192 GLICE (R/V Sanna, August 2022) ice collection was conducted as per other regions close to the outflow
193 of Sermeq Kujalleq (also known as Jakobshavn Isbræ) and Eqip Sermia (Supp. Table 1). Additionally,

194 ice fragments were collected from two large icebergs in Disko Bay, referred to herein as fragments from
195 Iceberg "Beluga" and Iceberg "Narwhal". These icebergs were tracked using the ship's radar by logging
196 the coordinates and relative bearing of the approximate centre of the iceberg at regular time intervals. In
197 Nuup Kangerlua (southwest Greenland), samples were collected on 5 repeated campaigns spanning boreal
198 spring and summer in different years (May 2014, July 2015, August 2018, May 2019 and September
199 2019) to assess the reproducibility of data from the same region by different teams deploying the same
200 methods in different months and years.
201

202 **2.2 Sediment load measurements**

203 Wet sediment sub-samples were dried at 60°C to determine sediment load (dry weight of sediment per
204 unit volume, mg L⁻¹). Sediment load was determined for a subset of randomly collected ice samples in
205 parallel with (micro)nutrients in the Antarctic Peninsula. In Maxwell Bay (King George Island), a targeted
206 exercise was conducted to collect ice with embedded sediment. Eight large ice fragments (10-45 kg) with
207 sediment layers embedded within the ice were retained in sealed opaque plastic boxes. These fragments
208 were specifically selected to avoid the possibility of including samples with surface sediment acquired by
209 ice scouring the coastline or shallow sediments. Boxes were half-filled with seawater from the bay.
210 Sediment-rich ice was left to melt in the dark with an air temperature of ~5-10°C. Periodically (after 2, 4,
211 8, 16, 24, and 48 hours) the water was weighed and settled sediment was removed by decanting and
212 filtration before estimating its dry weight.
213

214 **2.3 Chemical measurements**

215 Dissolved trace metal samples were acidified after filtration to pH 1.9 by addition of 180 µL HCl (UPA,
216 ROMIL) and allowed to stand upright for >6 months prior to analysis. Unfiltered trace metal samples
217 were acidified similarly and trace metals in these samples are subsequently referred to as 'total
218 dissolvable'; defined as dissolved metals plus any additional metals present which are soluble at pH 1.9
219 after 6 months of storage. Analysis via inductively-coupled, plasma mass spectrometry (ICP-MS, Element
220 XR, ThermoFisher Scientific) was undertaken after dilution with indium-spiked 1 M HNO₃ (distilled in-

221 house from SPA grade HNO₃, Roth). 4 mL aliquots of total dissolvable samples were filtered (0.2 μm,
222 polyvinyl difluoride, Millipore) immediately prior to analysis.

223
224 Calibration for Fe and Mn was via standard addition with a linear peak response from 1–1000 nM ($R^2 >$
225 0.99). Analysis of the reference material CASS-6 yielded a Fe concentration of 26.6 ± 1.2 nM (certified
226 27.9 ± 2.1 nM) and a Mn concentration of 37.1 ± 0.83 nM (certified 40.4 ± 2.18 nM). Due to the very
227 broad range of Fe concentrations in ice samples, samples were run using varying dilution factors.
228 Precision is improved at low dilution factors so we report results from the lowest dilution factor that could
229 be used to keep Fe and Mn concentrations within the calibrated range (in many cases dissolved samples
230 could be run without dilution). Dissolved samples were initially run at a tenfold dilution, using 1 M HNO₃.
231 A 1 M HNO₃ blank from the same acid batch was analysed every 10 samples and in triplicate at the start
232 and end of each sample rack (90 × 4 mL sample vials). Total dissolvable samples (unfiltered, acidified
233 samples) were initially run at a hundredfold dilution followed by a tenfold dilution for samples with
234 nanomolar concentrations. Samples with measured concentrations of Fe or Mn <25 nM were then re-run
235 without dilution. Detection limits, assessed as 3 standard deviations of blank (1 M HNO₃) measurements,
236 varied between batches (and dilution factors) but were invariably <0.86 nM dFe and <0.83 nM dMn for
237 the standard tenfold dilution analyses. The field blank (deionized water filtered and processed as a sample)
238 was below the detection limit. As in a majority of cases samples were run by dilution, the 1 M HNO₃ acid
239 used to both dilute samples and run as a reagent blank every 10 samples was therefore considered the
240 most useful blank measurement. Mean (±standard deviation) blank (1 M HNO₃) measurements varied by
241 acid batch from 0.06 ± 0.02 nM dFe, 0.03 ± 0.02 nM dMn; to 0.38 ± 0.08 nM dFe, and 0.14 ± 0.08 nM
242 dMn.

243
244 Where macronutrient samples were not collected in parallel with trace metals, samples preserved for trace
245 metals were analysed for PO₄³⁻ and dSi (this was not possible for NO_x⁻ because of residual contamination
246 from concentrated HNO₃ in LDPE bottles). Analysis of macronutrients was conducted for NO₃⁻, NO₂⁻,
247 PO₄³⁻ and dSi by segmented flow injection analysis using a QUAATRO (Seal Analytical) auto-analyzer
248 (Hansen and Koroleff, 1999). Recoveries of a certified reference solution (KANSO, Japan) were $98 \pm 1\%$

249 NO_x^- , $99 \pm 1\%$ PO_4^{3-} and $97 \pm 3\%$ dSi. Detection limits varied between sample batches and were <0.10
250 $\mu\text{M NO}_x^-$, $<0.02 \mu\text{M NO}_2^-$, $<0.10 \mu\text{M PO}_4^{3-}$, and $<0.25 \mu\text{M dSi}$.

251

252 **2.4 Data compilation**

253

254 In addition to new data from 367 new samples collected and analysed herein, existing comparable data
255 was compiled from prior literature, most of which was processed in prior work by the same protocol in
256 the same laboratories as herein (see Supp. Table 1). Inclusive of prior work, a total of 589 samples are
257 available for interpretation (note that not all samples were analysed for all parameters so n varies between
258 statistical analyses). Previously published data includes samples from Greenland, Svalbard, the Antarctic
259 Peninsula, Patagonia and Iceland (De Baar et al., 1995; Campbell and Yeats, 1982; Forsch et al., 2021;
260 Höfer et al., 2019; Hopwood et al., 2017, 2019; Lin et al., 2011; Loscher et al., 1997; Martin et al., 1990b).
261 Altogether, 575 out of the 589 samples reported were collected and analysed as described herein at the
262 same laboratories. Only 14 literature values were from other laboratories so there is a high degree of
263 internal consistency in the methods used. Throughout concentrations are reported in units L^{-1} , referring
264 to the concentration measured in meltwater.

265 **2.5 Statistical analysis**

266

267 To test if icebergs had statistically significant regional differences in (micro)nutrient concentrations
268 depending on their origin at a hemisphere, regional or catchment scale, a multivariate PERMANOVA
269 was realized (function `adonis2` from `vegan` package, Oksanen et al., 2020) using the concentrations of
270 trace metals (both dissolved and total dissolvable) and macronutrients (NO_x^- , PO_4^{3-} and dSi). Along with
271 this analysis a non-metric MultiDimensional Scaling (nMDS, function `metaMDS` from `vegan` package,
272 Oksanen et al., 2020) was used to compute the ordination of the iceberg samples depending on their
273 nutrient concentrations. An nMDS is an unconstrained ordination analysis that assess the
274 similarities/dissimilarities among datapoints only using the set of variables informing the ordination
275 (herein macro- and micronutrients concentrations). The variables considered for the analysis are

276 summarized in orthogonal dimensions showing the more similar datapoints as closer (groupings of
277 datapoints with similar characteristics) within the space created by the orthogonal dimensions. The same
278 analyses were used to assess differences in Disko Bay samples collected in August 2022, in this case
279 comparing iceberg samples collected in inshore (<1 km from the coastline) and offshore (>15 km from
280 the coastline) zones. In both cases subsequent ANOVA (aov function package stats) and a Tuckey test
281 (TukeyHSD function package stats) were undertaken to test for significant differences in specific
282 (micro)nutrient concentrations.

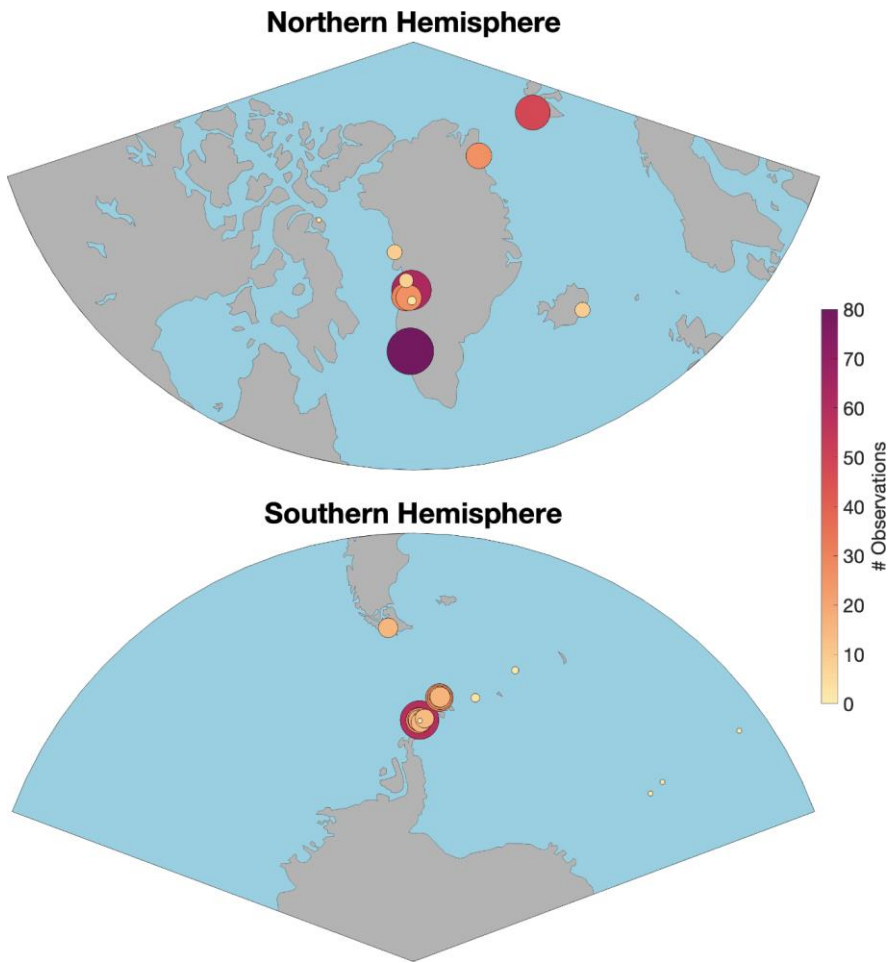
283
284 The relationship between iceberg sediment load and the concentration of trace metals (both dissolved and
285 total dissolvable) and macronutrients was determined by means of a linear regression (lm function
286 package stats). For this analysis two outliers were removed from the dataset because their sediment load
287 values were over an order of magnitude larger (50726 mg L⁻¹ and 6128 mg L⁻¹) than other values (total
288 n=144); including these two data points would have disproportionately skewed the relationships. Finally,
289 to analyse how melting and sediment release rates changed over time using the incubations in Maxwell
290 Bay, we used the same procedure as Höfer et al., (2018). In short, we first tested if the relationship between
291 melting and sediment release rates and time better fitted a linear or exponential relationship using a
292 second-order logistic regression. Then, we tested the fit of the selected relationship (exponential in this
293 case) to see if the relationship was significant and determined the percentage of variance explained (lm
294 function package stats). Since the initial conditions of each incubation (i.e. iceberg size, shape and initial
295 sediment load) varied, the rates for each individual experiment were normalized by dividing each rate by
296 the maximum rate registered in the same incubation. All statistical analyses and figures (package ggplot2)
297 were realized using R version 4.3.2 (R Core Team, 2023).

298 **3 Results**

299 **3.1 Nutrient distributions in the global iceberg dataset**

300 A total of 589 ice fragments have been analysed to date. The combined data is more balanced compared
301 to prior work in terms of coverage of Antarctica (45% of samples), Greenland (42% of samples), Svalbard
302 (8.1% of samples), and smaller sub-polar catchments in Patagonia, Canada, and Iceland (4.2% of

303 samples). There are however still some spatial biases in the data. Notably samples from Greenland are
304 largely from the west (Fig. 1), and samples from Antarctica are all from the Antarctic Peninsula or
305 downstream waters along the “Iceberg Alley” in the Weddell Sea and the South Atlantic sector of the
306 Southern Ocean (Tournadre et al., 2016). Almost all samples were collected in summer, with only a subset
307 of samples (from Nuup Kangerlua, Supp. Table 4) collected in spring and autumn to investigate potential
308 seasonal changes. At the catchment scale, Nuup Kangerlua (southwest Greenland, also known as
309 Godthåbsfjord, 15% of the dataset), Eqip Sermia (west Greenland, 11% of the dataset), Thunder Bay
310 (Western Antarctic Peninsula, 10% of the dataset), Kongsfjorden (Svalbard, 8.2% of the dataset), Disko
311 Bay (west Greenland, 5.1% of the dataset), and Nelson Island (Northern Antarctic Peninsula, 5.1% of the
312 dataset) are particularly well represented. The other 23 catchments each account for <5% of the samples.
313



314

315

316 Figure 1. Sample distributions in the Northern and Southern Hemispheres. Literature values from prior

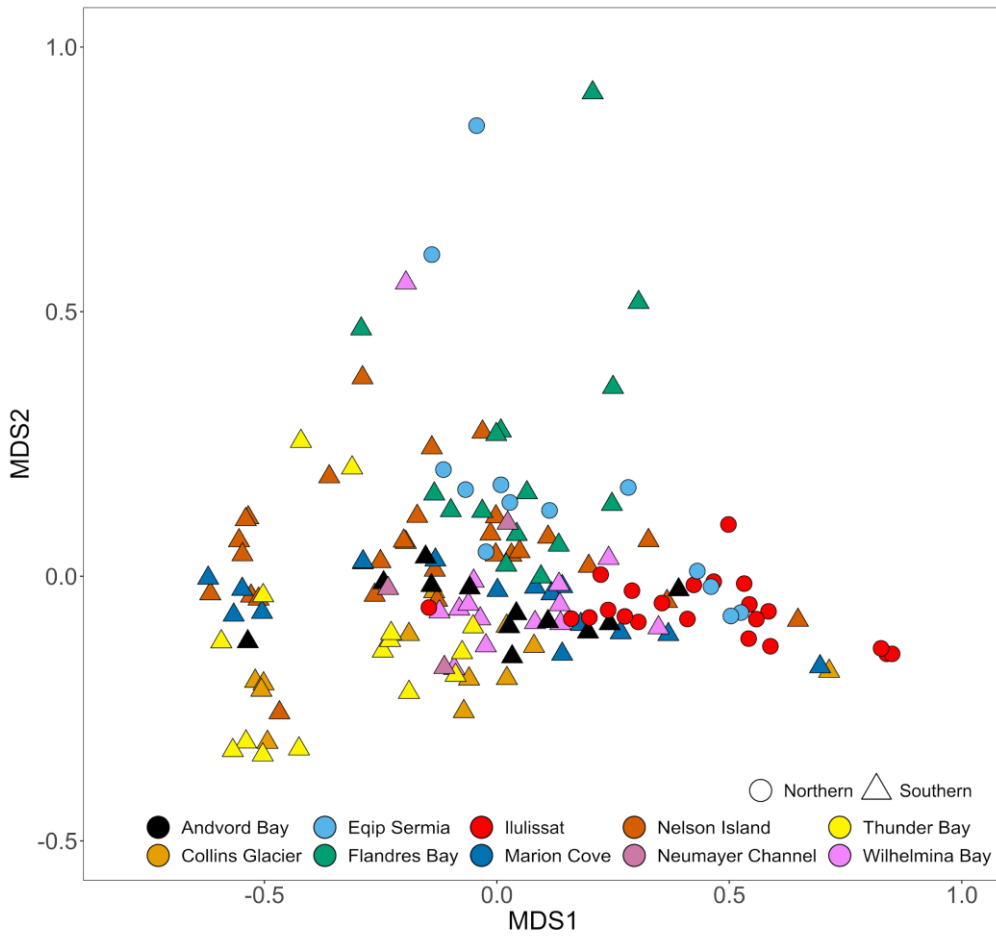
317 work are included (see Supp. Table 1 for a full list of details).

318

319 Average macronutrient concentrations in ice samples were low with median concentrations of 0.04 μM
320 PO_4^{3-} , 0.54 μM NO_3^- and 0.02 μM dSi. Throughout the dataset NO_2^- was close to, or below, detection
321 thus NO_3^- and NO_x^- concentrations were practically identical with NO_2^- almost invariably constituting
322 <10% of NO_x^- (mean 1.8%). Mean nutrient concentrations in all cases were higher than median
323 concentrations and the large relative standard deviations indicated that variability between samples might
324 mask any regional differences. Preliminary analysis revealed a large fraction of data below detection (i.e.
325 concentrations <LOD) for several components particularly PO_4^{3-} (24% of all measurements <LOD) and
326 dSi (48% if all measurements <LOD). Other (micro)nutrients were less affected by detection limits, e.g.
327 only 8% of NO_x concentrations were <LOD. In any dataset with a large fraction of data <LOD, how these
328 values are treated makes some difference to calculated statistics so reported averages vary for PO_4^{3-} and
329 dSi depending on how LOD values are treated. Removing values <LOD entirely would skew the statistical
330 analyses. For example, the median values reported above increase from 0.04 to 0.05 μM PO_4^{3-} , and 0.02
331 to 0.19 μM dSi if values <LOD are excluded. For consistency throughout all statistical analyses, a value
332 of '0' was therefore used to represent LOD data.

333
334 It has been previously reported that both TdFe and dFe concentrations are extremely variable within ice
335 samples collected at the same location (Hopwood et al., 2017; [Lin and Twining, 2012](#); Lin et al., 2011).
336 This remained the case with the expanded dataset herein with notable differences between the mean (82
337 nM dFe, 13 μM TdFe) and median concentrations (12 nM dFe, 220 nM TdFe) on a global scale. An
338 extremely broad range of concentrations was also observed for both dissolved Mn (mean 26 nM, median
339 2.6 nM) and total dissolvable Mn (TdMn; mean 150 nM, median 10 nM). As per Fe, this reflected the
340 skewed distribution of the dataset towards a low number of samples with extremely high concentrations.
341 The highest 2% of TdMn samples accounted for 79% of the cumulative TdMn measured. Similarly, the
342 highest 2% of TdFe samples accounted for 77% of the cumulative TdFe measured. Accordingly, there
343 were very high relative standard deviations for both mean dMn (26 ± 160 nM) and TdMn (150 ± 1500
344 nM) which, as per Fe, remained high when data was grouped by region or catchment. Considering all
345 (micro)nutrients measured, there were no significant differences in the iceberg chemical composition at
346 a hemispheric (p value = 0.16) or regional (p value = 0.16) level. However, a PERMANOVA analysis

347 showed significant differences ($R^2 = 0.24$, p value < 0.001) at a catchment level. Similarly, an nMDS
348 analysis (stress = 0.07) showed that samples from the same catchment tended to be grouped closer
349 together (Fig. 2) and in general Antarctic samples were distributed on the left side, whereas Arctic samples
350 were more abundant on the right side of the ordination analysis (Fig. 2).

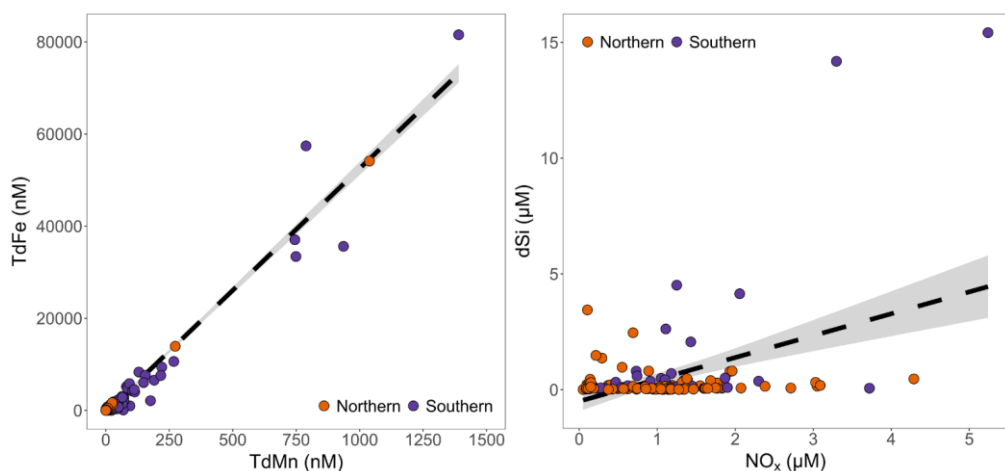


351

352 Figure 2. A scatter plot showing the results of an nMDS ordination analysis using macro- and
353 micronutrient concentrations. Only samples with complete data for the following parameters are shown:
354 NO_x^- , PO_4^{3-} , dSi, dFe, TdFe, dMn and TdMn. A non-metric MultiDimensional Scaling (nMDS) ordination
355 is used to represent multi-dimensional data in a reduced number of dimensions. MDS1 and MDS2 are
356 multidimensional scaling factors which represent the dissimilarities between the data sorted to catchment
357 level. Datapoints represent individual samples. Datapoints which appear further apart are more different,
358 whereas those that cluster together are more similar. A PERMANOVA analysis of iceberg nutrient
359 concentrations showed significant differences at a catchment level ($R^2 = 0.24$, p value <0.001). Shapes
360 denote hemispheres, while colours denote specific sampling locations.

361
362 The ratio of TdFe:TdMn was linear ($R^2 = 0.95$, calculated excluding the highest 2% of Mn and Fe
363 concentrations to avoid skewing the gradient, Fig. 3). Furthermore, the total dissolvable Mn:Fe ratio of
364 0.02~~325~~ (linear regression $\text{TdMn} = 0.02\text{325} \times [\text{TdFe}]$) was close to mean continental crust composition
365 which is approximately 0.1% MnO and 5.04% FeO by weight (producing a ratio of 0.020) (Rudnick and
366 Gao, 2004). In contrast, no clear relationship was observed between dFe and dMn. For all data, all
367 Antarctic data and all Greenlandic data, respectively, the mean dMn:dFe (0.47, 0.50 and 0.28) and median
368 dMn:dFe (0.17, 0.19 and 0.11) ratios were however consistently higher than the TdMn:TdFe ratio. This
369 indicates an excess of dMn compared to the lithogenic ratio observed in the total dissolvable fraction.

370
371 Neither dMn or dFe correlated well with dSi. Throughout the whole dataset, dSi concentrations were low.
372 Only 7 of 478 samples had dSi concentrations $>10 \mu\text{M}$, only 9.4% of samples had concentrations >1.0
373 μM , and 48% of all samples were below detection. Dissolved Si therefore had concentrations and a
374 distribution much more like NO_x^- and PO_4^{3-} than Mn or Fe. This was not typically the case in glacier
375 runoff close to the sites where ice was collected (Supp. Table 2). With the exception of subglacial runoff
376 collected on Doumer Island (South Bay, Western Antarctic Peninsula), dSi concentrations in runoff were
377 always high relative to both nitrate in runoff (typically $\sim 12 \times [\text{NO}_x^-]$) and to the mean dSi concentration
378 in icebergs. Doumer Island consists of a small ice cap which is likely cold-based with steep topography,
379 such that subglacial chemical weathering runoff sediment interaction is probably likely limited.



380

381 Figure 3. A comparison of (micro)nutrient concentrations in all ice fragments where concentrations were
 382 above the detection limits. *Left* Total dissolvable Fe and total dissolvable Mn were strongly correlated (p
 383 value <0.001 , $R^2 = 0.95$), note the highest 2% of measured concentrations were excluded to avoid skewing
 384 the gradient. *Right* dSi and NO_x^- had a weak correlation (p value <0.001 , $R^2 = 0.19$). The 95% confidence
 385 interval is shaded in grey.

386

387 No significant relationship was evident between PO_4^{3-} and NO_x^- concentrations, whereas a weak, but
 388 significant, relationship was evident between dSi and NO_x^- concentrations (Fig. 3). A subset of samples
 389 appeared to show a close to 1:1 relationship between dSi and NO_x^- , which resembles the Redfield Ratio
 390 (Redfield, 1934). A closer inspection of these points shows they accounted for about 14% of the sub-
 391 dataset where all macronutrient concentrations were detectable ($n=22$ for those with $[\text{NO}_x^-]$ and $[\text{dSi}] >0.4$
 392 μM , for lower concentrations it is largely arbitrary determining whether or not samples can be assigned
 393 to the group). Samples in this group include multiple catchments but with a large component from Ilulissat
 394 (32% of datapoints) and Nuup Kangerlua (55% of datapoints), both of which were over-represented
 395 compared to their proportional importance in the sub-dataset where they each constituted 18% of
 396 datapoints. Antarctic samples and samples from Eqip Sermia were under-represented in this ~1:1 group,

397 accounting for 0 and 2 (9%) samples, respectively, despite contributing 26% and 20% of the samples with
398 all macronutrients detectable. The ~1:1 datapoints all refer to summertime so cannot easily be explained
399 as mistaken sea ice samples. Furthermore, observed nutrient concentrations were often too high to be
400 explained by carry-over from seawater contamination (see Section 3.2). The ratios of dSi: NO_3^- also did
401 not consistently match the ratio in near-surface fjord water samples where this was collected in parallel
402 with icebergs. Whilst the dSi: NO_3^- ratio in most near-surface samples from the Ilulissat Icefjord in August
403 2022 was ~1 (1.39 ± 0.61 , $n=25$ in August 2022), for Nuup Kangerlua in August and September 2019 the
404 ratio of dSi: NO_3^- was always >18 (Krause et al., 2021). A ~1:1 NO_x^- :dSi ratio in ice nevertheless
405 resembles a marine origin.

406 **3.2 Evaluating reproducibility and potential sampling biases**

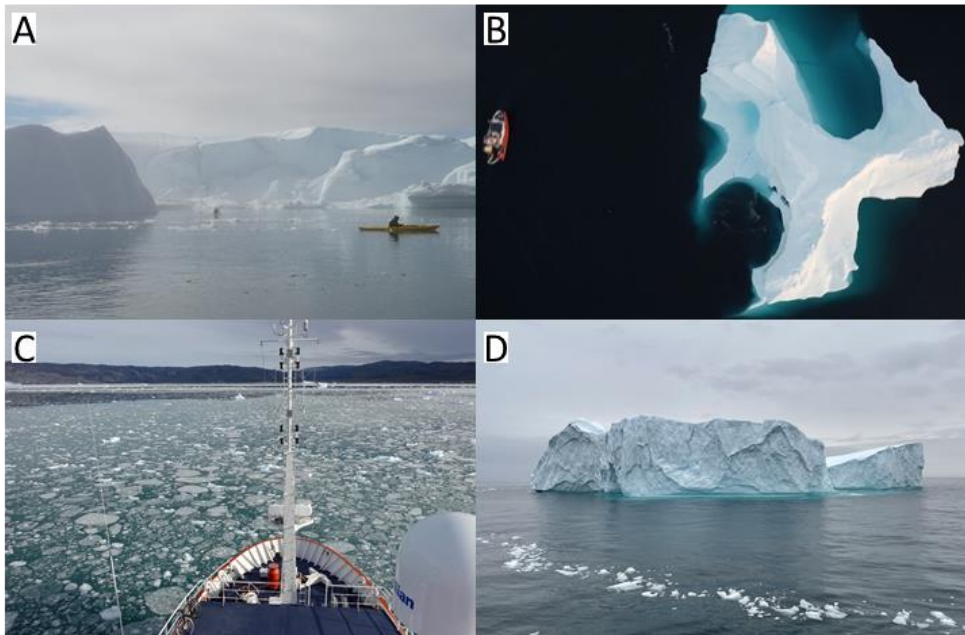
407 Glacial ice can usually be visually distinguished from sea ice due to its distinct texture, colour and
408 morphology. For meltwater samples that were tested for salinity, values were always <0.3 psu. However,
409 even minor traces of seawater in samples would be sufficient to impart a measurable macronutrient
410 concentration change because ice macronutrient concentrations were generally very low compared to
411 pelagic macronutrient concentrations in the corresponding sampling regions. This is particularly the case
412 at the Antarctic sample sites where high macronutrient concentrations of 20-80 μM dSi, 1-2 μM PO_4^{3-}
413 and 10-30 μM NO_3^- are relatively typical of marine waters (e.g. Höfer et al., 2019; Forsch et al., 2021;
414 Trefault et al., 2021). Close to marine-terminating glaciers in the Arctic, macronutrient concentrations in
415 near-surface waters can still be elevated relative to the low concentrations reported for ice, e.g. 1-30 μM
416 dSi, 0.2-0.7 μM PO_4^{3-} and 0-10 μM NO_3^- for the inner part of Nuup Kangerlua (Krause et al., 2021; Meire
417 et al., 2017). Thus, seawater macronutrient concentrations were generally equal to, or greater than ice
418 concentrations at the locations where ice calves.

419
420 Using the maximum observed marine macronutrient concentrations for our Antarctic sampling locations,
421 assuming no detectable macronutrients in ice and that salinity of 0.3 exclusively reflected the carry-over
422 of seawater from sampling, nutrient concentrations of up to 0.26 μM NO_3^- , 0.02 PO_4^{3-} μM and 0.069 μM
423 dSi could be observed as a seawater contamination signal. The rinsing procedure used to collect samples

424 herein whereby ice was sequentially melted, with the meltwater then used to swill and rinse the sample
425 bag, was designed ~~precisely~~ to minimize trace metal contamination and three such rinses undertaken
426 correctly would theoretically remove ~99.99% of any saline water collected with an ice sample in addition
427 to any contamination from ice handling. This would also not leave a detectable (>0.01) salinity increase
428 in the collected sample such that any detected salinity would have to come from ice melt. Sea ice samples
429 were not targeted for sampling herein, but two samples were collected during the 2017 Pia fjord campaign
430 (Patagonia) alongside calved ice samples and measured macronutrient concentrations were: 2.00 and 5.97
431 $\mu\text{M NO}_x^-$, 0.08 and 0.13 $\mu\text{M PO}_4^{3-}$, 0.28 and 0.63 $\mu\text{M dSi}$. These sea ice NO_x^- and dSi concentrations
432 were above average compared to freshwater ice samples collected in the same location (Supp. Table 2).
433 Similarly, samples of land fast sea ice from Antarctica generally have high concentrations of all
434 macronutrients compared to iceberg samples reported herein (Grotti et al., 2005; Günther and Dieckmann,
435 1999; Nomura et al., 2023). ~~It is apparent from T~~the ratio of NO_x^- : PO_4^{3-} :dSi in sea ice is strong evidence
436 ~~that nutrients~~the high nutrient concentration in sea ice have a primarily saline origin (Henley et al., 2023).
437 Sampling protocols for sea ice are however different in several aspects particularly the application of a
438 sequential rinsing (for glacial ice, but not for sea ice) and ambient temperatures during sample collection.
439 A sequential rinsing with sea ice, as applied herein, might lead to an uneven distribution of nutrients in
440 meltwater samples due to the layered structure of sea ice and the effects of brine channels (Ackley and
441 Sullivan, 1994; Gleitz et al., 1995; Vancoppenolle et al., 2010). With the possible exceptions of regions
442 that experience ice mélange (a mixture of sea ice and icebergs) and/or marine ice, glacial ice is expected
443 to be more homogenous with respect to salinity. ~~In prior work we also demonstrated no sustained trend~~
444 ~~in Fe concentrations when aliquots of meltwater were collected from ice fragments in series (Hopwood~~
445 ~~et al., 2016). A further critical difference with sea ice samples concerns ambient conditions as all ice~~
446 ~~samples collected herein were obtained from seawater with temperatures >0°C i.e. under conditions where~~
447 ~~ice was melting when it was collected. Conversely, a large fraction of sea ice cores studied to date refer~~
448 ~~to conditions without *in situ* melt occurring (Henley et al., 2023).~~

449
450 During the dedicated iceberg cruise campaign GLICE in Disko Bay (August 2022), ice collection was
451 confined to 4 subregions of interest (Fig. 4, Supp. Table 3). There was partial ice cover in Disko Bay

452 during boreal summer, which was mainly limited to a patch of high iceberg density close to the outflow
453 of Ilulissat Icefjord. Combined with the confined nature of the coastal fjords sampled and the relatively
454 fast disintegration of smaller ice fragments, it was possible to identify with a high degree of certainty the
455 origin of ice within each subregion (Fig. 4). Within the fjord system hosting the marine-terminating
456 glacier Equip Sermia, ice fragments were highly likely to have originated from either Equip Sermia itself
457 or, if not, from adjacent calving fronts in the same fjord. Similarly, close to the outflow of Ilulissat
458 Icefjord, ice fragments were highly likely to have originated from Sermeq Kujalleq. Ice slicks which were
459 visibly observed to calve from two offshore icebergs within an hour prior to sample collection each
460 constituted an additional subregion of interest. The two icebergs, referred to herein as ‘Narwhal’ and
461 ‘Beluga’ were both isolated from other floating ice features with maximum dimensions above the
462 waterline of >100 m width and >20 m height (Fig. 4). Radar measurements determined that ‘Narwhal’
463 was approximately stationary throughout the observation period (~12 hours) likely pirouetting on an area
464 of shallow bathymetry. Iceberg ‘Beluga’ was free-floating and proceeding northwards along a trajectory
465 through the area which hosted the highest observed iceberg densities in Disko Bay over the cruise duration
466 (mid-August 2022).



467

468 Figure 4. Ice sample collection areas in four distinct regions of Disko Bay. A Icebergs grounded on the
 469 sill at the entrance to the Ilulissat Icefjord. B An offshore iceberg which was grounded during the sampling
 470 period referred to herein as iceberg 'Narwhal'. C Ice fragments in front of the marine-terminating glacier
 471 Eqip Sermia. D An offshore iceberg which was free-floating during the sampling period referred to herein
 472 as iceberg 'Beluga'.

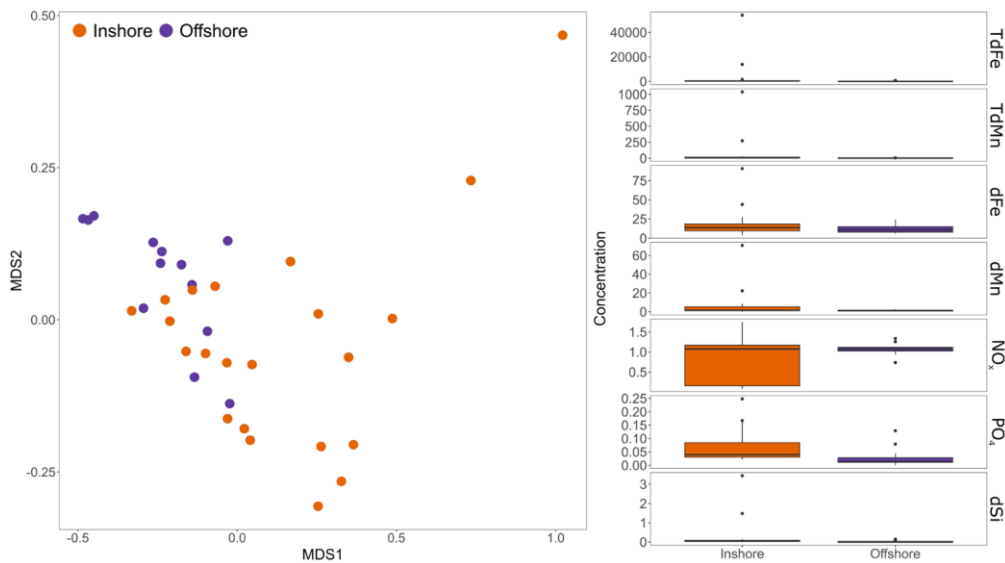
473

474 Ice from the 4 sampled subregions in Disko Bay was similar in all cases with overlapping ranges for the
 475 NO_x^- , PO_4^{3-} and dSi concentrations of ice at different locations (Fig. 5). A PERMANOVA analysis
 476 showed small, but significant, differences ($R^2 = 0.15$, p value = 0.002) in the chemical composition of
 477 iceberg samples collected inshore (Groups A and C, Fig. 4) or offshore (Groups B and D, Fig. 4) in Disko
 478 Bay when combining groups. An ordination analysis (nMDS stress = 0.04) showed that offshore icebergs
 479 were grouped together on the left side of the ordination, whereas inshore icebergs were more common on

480 the right side of the ordination (Fig. 5). In general, offshore and inshore icebergs presented similar
481 concentrations of all nutrients in most of the samples, except for a few inshore samples that had higher
482 concentrations of all nutrients (Fig. 5). When testing these differences for each individual nutrient, only
483 PO_4^{3-} showed significant differences between the two categories (p value = 0.035), with offshore icebergs
484 showing lower concentrations (Fig. 5). The difference between inshore and offshore ice, whilst present,
485 was therefore relatively modest.

486

487 Further insight can be gained from a comparison of all data available from Nuup Kangerlua, a relatively
488 well-studied glacier fjord in southwest Greenland. The fjord hosts three marine-terminating glaciers with
489 heavy ice mélange cover observed in the inner fjord year-round and some sea ice in the inner fjord during
490 winter. Samples were collected from the fjord during five independent field campaigns from 2014 to 2019
491 in different seasons from May in boreal spring to September in boreal autumn. Considering the number
492 of parameters sampled and the relatively high standard deviation of almost all parameters relative to the
493 mean or median measured concentrations, there was limited evidence for any seasonal or inter-campaign
494 differences (Supp. Table 4). No significant differences ($p > 0.05$) were found between groups of samples
495 obtained at the same field site when organizing the complete dataset by field site and defining each
496 separate field campaign as a group.



497

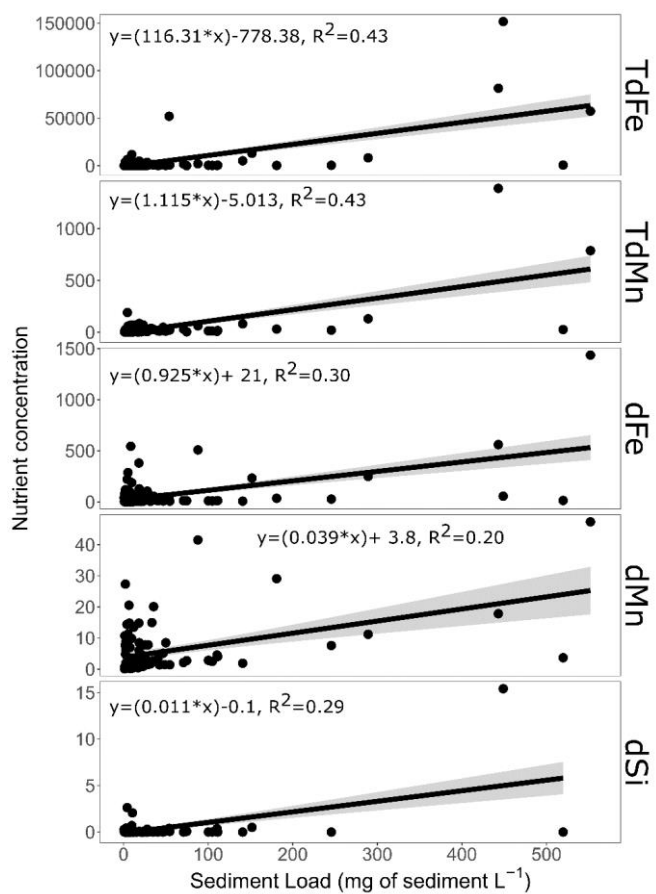
498 Figure 5. Comparison of nutrient concentrations from inshore and offshore ice samples collected in Disko
 499 Bay (August 2022, see Fig. 4). *Left* An ordination analysis (nMDS) comparing concentrations of all
 500 nutrients measured in ice contrasting inshore and offshore areas of Disko Bay. Inshore samples were
 501 collected within 1 km of the coastline, whereas offshore values were all from >15 km away from the
 502 coastline. A PERMANOVA analysis of iceberg nutrient concentrations showed weak but significant
 503 differences between both areas ($R^2 = 0.15$, p value = 0.002). *Right* A direct comparison of all nutrient
 504 concentrations for the same dataset. Units: μM for dSi, NO_x^- and PO_4^{3-} ; nM for all trace metals. Only
 505 PO_4^{3-} showed a significant difference between the two categories (p value = 0.035).

506 3.3 Sediment load within icebergs and its relationship with nutrient concentration

507 The sediment load within icebergs collected around the Antarctic Peninsula was highly variable with a
 508 maximum of 5072 mg L^{-1} and a minimum of 0.69 mg L^{-1} (median 8.5 mg L^{-1} and mean 430.5 mg L^{-1}).
 509 Particle loads were assessed in three Antarctic locations. The median dry mass was similar across three
 510 areas, but the mean (\pm standard deviation) dry mass was more variable due to the occasional sample with

511 a high sediment load. Mean dry masses across three areas were: Maxwell Bay, King George Island, (n=65)
512 $910 \pm 6300 \text{ mg L}^{-1}$; Thunder Bay and Neumayer Channel, Wiencke Island, (n=19) $35 \pm 110 \text{ mg L}^{-1}$; and
513 South Bay, Doumer Island, (n=60) $39 \pm 98 \text{ mg L}^{-1}$. Median sediment loads in the three regions were 12,
514 2.5 and 7.7 mg L^{-1} , respectively. The heterogeneous distribution of sediments was reflected in the fact
515 that ~2% of samples collected contributed ~90% of the total sediment retrieved from the iceberg samples
516 collectively (Fig. 6). This distribution is similar to previous analysis regarding TdFe (Hopwood et al.,
517 2019), and sediment load in icebergs from Svalbard (Dowdeswell and Dowdeswell, 1989) Hopwood et
518 al., 2017). It also qualitatively matches the distribution of TdMn and TdFe observed herein (see Section
519 3.1).

520
521 As Fe, Mn and dSi might have sedimentary origins, we tested if there were any significant relationships
522 between the sediment load of an iceberg and the concentration of each macronutrient and both total
523 dissolvable and dissolved trace metals (Fig. 6). For NO_x^- and PO_4^{3-} there was no significant relationship
524 between sediment load and concentration (p values of 0.18 and 0.26 respectively). ~~This is consistent with~~
525 ~~the hypothesis that these nutrients primarily have an atmospheric deposition origin which contributes only~~
526 ~~a minor fraction of the sediment load to bulk ice.~~ Conversely, TdFe, TdMn, dFe, dMn and dSi all had
527 significant relationships with sediment load. The concentrations of the total dissolvable fraction of trace
528 metals showed better fits (TdFe $R^2 = 0.43$, p value <0.001 ; TdMn $R^2 = 0.43$, p value <0.001), than the
529 dissolved phases of metals (dFe $R^2 = 0.30$, p value <0.001 ; dMn $R^2 = 0.20$, p value <0.001) and dSi (R^2
530 $= 0.28$, p value <0.001). This is consistent with the expectation that englacial sediment drives a direct
531 enrichment in TdFe and TdMn, which increase proportionately with sediment load. The enrichment of
532 dFe, dMn and dSi is more variable and may depend on the specific conditions that sediment and ice
533 experience between englacial sediment incorporation and sample collection.



534

535

536

537

538

539

Figure 6. Iceberg sediment load and its relationship with nutrient concentrations. *Left* The uneven release of sediment in randomly collected ice samples from the Antarctic Peninsula. *Right* The relationship between nutrient concentrations and sediment load for ice samples from the Antarctic Peninsula (no samples from elsewhere determined sediment load on the same ice fragments as nutrient concentrations).

540 Only significant (p value <0.001) relationships are shown. No significant relationship was evident for
541 sediment load with nitrate or phosphate. Units: μM for dSi, nM for all trace metals.

542
543 On several occasions in Nuup Kangerlua and Maxwell Bay we observed structures up to several
544 centimetres wide/deep on iceberg surfaces akin to cryoconite holes both above and below the waterline.
545 The sediment within such holes was easily disturbed ~~when approaching ice fragments~~. The regular
546 agitation and movement of floating ice fragments and the chaotic nature of calving events suggests that
547 cryoconite holes on icebergs formed *in situ* rather than being relics of a glacier surface prior to calving.
548 This raises an interesting question about whether sediment-rich layers and any associated nutrients could
549 be subject to disintegration mechanisms distinct from bulk ice. When large ice samples weighing 10-45
550 kg were stored in the dark at 5-10°C, higher loads of sediment were released in the initial melt fractions
551 (Supp. Fig. 1). This trend was highly reproducible occurring in all observed experiments (n=8) when large
552 ice samples specifically targeted for their high englacial sediment loads were retained. The sediment
553 release rate declined with an exponential logarithmic function over the first 48 hours (Supp. Figure 1). It
554 should be noted that randomly collected samples had much lower sediment loads ~~(Fig. 6)~~.

555 4 Discussion

556 4.1 Insights into nutrient origins from ratios

557 There are several distinct mechanisms via which ice could accumulate different nutrient ratios.
558 Precipitation and aerosol deposition on ice surfaces ~~will contribute to the~~ ~~would be expected to deposit~~
559 ~~NO_x^- and PO_4^{3-} concentrations present in the ice matrix~~ (Fischer et al., 1998; Kjær et al., 2015), assuming
560 a limited biogeochemical imprint from surface biological (or photochemical) processes. ~~Atmospheric~~
561 ~~deposition of NO_x^- and PO_4^{3-} varies regionally. Snow NO_3^- deposition over central Greenland is reported~~
562 ~~as $1.21 \pm 0.19 \mu\text{mol kg}^{-1}$ for recent and $0.56 \pm 0.19 \mu\text{mol kg}^{-1}$ for pre-industrial values (Fischer et al.,~~
563 ~~1998). Reported concentrations of PO_4^{3-} are more sensitive to the method used due to universally low~~
564 ~~concentrations.~~ Phosphate concentrations in ice from the last glacial period in Greenland are reported to
565 range from 3 to 62 nM (Kjær et al., 2015). These ranges are similar to the NO_3^- and PO_4^{3-} values we report
566 for Greenlandic calved ice herein: mean (\pm standard deviation) $0.78 \pm 0.69 \text{NO}_3^-$, median 0.74NO_3^- , mean

567 36 ± 50 nM PO_4^{3-} , and median 28 nM PO_4^{3-} . Modern atmospheric deposition is expected to impact the
568 N:P ratio as atmospheric pollution is generally associated with higher N:P ratios (e.g. Peñuelas et al.,
569 2012) and could explain the increase in N:P ratio at higher NO_3^- concentrations. ~~Atmospheric deposition~~
570 ~~of NO_3^- is~~ Antarctica is less directly affected by anthropogenic emissions, but the ranges of NO_3^- reported
571 for snow and ice samples overlap with the corresponding values for Greenland e.g. ranges of 0.08-2.12
572 μM (Akers et al., 2022) and 0.29-2.58 μM (Neubauer & Heumann., 1988).

573
574 In addition to ~~an atmospheric deposition signal in ice~~ macronutrient concentrations in the ice matrix, ~~for~~
575 ~~NO_x^- and PO_4^{3-}~~ , some degree of sedimentary signal might also affect dSi concentrations due to release of
576 dSi from glacier-associated weathering processes (Halbach et al., 2019; Wadham et al., 2010). ~~In contrast~~
577 ~~no, or very limited, release of NO_3^- or PO_4^{3-} is expected from weathering which is supported by the~~
578 ~~correlations herein (Fig. 6)~~. Sediment associated with an iceberg could be from basal layers, other
579 englacial sediment entrained prior to calving, or acquired from scouring events subsequent to calving.
580 Shallow areas of all field sites herein had grounded icebergs. In Disko Bay during 2 weeks of cruise
581 observations in August 2022 for example, the majority of large (>100 m width above water line) icebergs
582 were observed to be grounded. In terms of TdFe, TdMn, dFe, dMn and dSi we hypothesize that two
583 categories of sediment may be distinguishable. Englacial sediment with little biogeochemical processing
584 should retain a TdFe:TdMn ratio which is close to the crustal abundance ratio of Fe:Mn, with low dFe,
585 dMn and dSi concentrations. Basal sediment layers, particularly from catchments with warm-based
586 glaciers, may have a similar TdFe:TdMn ratio but higher concentrations of dFe, dMn and dSi due to more
587 active biogeochemical processing in subglacial environments (e.g. Wadham et al., 2010; Tranter et al.,
588 2005). Finally, scoured sediments acquired after calving could constitute a broad range of compositions
589 considering the gradient in benthic conditions along glacier fjords (Laufer-Meiser et al., 2021; Wehrmann
590 et al., 2013) and may accordingly contain more biogenic and/or authigenic phases than englacial sediment.
591 These sediments may be highly variable in composition but should impart high TdFe and TdMn
592 concentrations, with varying Fe:Mn ratios, and high dFe, dMn and dSi concentrations. Basal sediments
593 and scoured sediments from fjord environments therefore probably cannot be distinguished
594 unambiguously from concentrations measured herein alone. Yet we can likely distinguish englacial

595 sediment from basal or scoured sediment. Dissolved Si concentrations were low across the whole dataset,
596 suggesting basal ice was a very small component of sampled ice. The linear relationship between TdFe
597 and TdMn across a wide range of observed concentrations also suggests minimal incorporation of
598 authigenic mineral phases and, in combination with low dSi, hints that basal ice from warm-based glaciers
599 is largely absent from this dataset. This is consistent with the expectation that basal layers are largely lost
600 prior to, or rapidly following, iceberg calving (Smith et al., 2019). In contrast, in runoff sampled close to
601 iceberg sampling regions, dSi concentrations were elevated (range 1.2-44 μM) and often considerably
602 higher than concentrations measured in ice melt (Supp. Table 2).

603

604 The weak, but significant, relationships with dSi, dFe, dMn and sediment load; and the stronger
605 relationships between TdFe and TdMn and sediment load are consistent both with a sedimentary origin
606 of these components and the caveats that further physical and/or biogeochemical processing mechanisms
607 have to be considered to fully explain the distributions of dSi, dFe and dMn (Fig. 6). As the concentrations
608 of NO_x^- and PO_4^{3-} were consistent with an ice matrixatmospheric origin, a varying concentration of dSi
609 from sedimentary sources could also easily explain the observed trend in the NO_x^- :dSi and PO_4^{3-} :dSi
610 ratios. Whilst elevated dFe and dMn concentrations in runoff reflect release of these phases from glacier-
611 derived sediments (Hawkings et al., 2020; Raiswell, 2011), the concentrations herein for ice melt were
612 not strongly correlated with each other or sediment load (Fig. 6). This could reflect the origin of dissolved
613 Fe and Mn from distinct, different mineral phases ;-Y- yet dFe concentrations generally correlate poorly
614 with other trace elements in aquatic environments due to rapid scavenging onto particle surfaces and rapid
615 aggregation of colloids (which are included within the '<0.2 μm ' definition of dissolved herein) (Zhang
616 et al., 2015). A poor correlation could also therefore reflect the tendency for inorganic dFe species to
617 become rapidly scavenged close to source (Lippiatt et al., 2010). Measured concentrations herein refer to
618 freshly collected meltwater so it is difficult to establish how dFe concentrations may have changed during
619 the ice melting process. Conversely, dMn species are more stable in solution, especially in the photic zone
620 (Sunda et al., 1983; Sunda and Huntsman, 1988), and this is often reflected in much higher dMn:dFe
621 ratios in proglacial aquatic environments than would be expected based on crustal abundances (e.g. van
622 Genuchten et al., 2022; Hawkings et al., 2020; Yang et al., 2022). Curiously, dSi also correlated poorly

623 with all metal phases. This again could simply reflect different mineral phases driving elevated dSi, dFe
624 and dMn concentrations (van Genuchten et al., 2022). Yet considering all of these elements (Si, Fe and
625 Mn) are expected to be released from labile phases present in glacier-derived sediments, at least within
626 specific regions some degree of correlation might be expected. Further work to quantify the rates of gross
627 and net dFe, dMn and dSi release under *in situ* conditions within ice and frozen sediment layers, could
628 perhaps elucidate processes via which net release of these components may be uncoupled. Photochemical
629 processes are particularly likely to affect Fe and Mn release (Kim et al., 2010; Kim et al., 2024), and the
630 scavenging potential of Mn and Fe species (van Genuchten et al., 2022) may also be important in terms
631 of how they interact with other dissolved and particulate components of the ice-sediment-meltwater
632 matrix.

633

634 **4.2 Key role of sediment-rich layers, and their disintegration, for nutrient release**

635 Several works have speculated that Arctic and Antarctic icebergs may have distinct differences in
636 sediment load, with the former generally having higher sediment loads ~~than the latter~~ (Anderson et al.,
637 1980). However, there are several observer biases in making such comparisons. Arctic icebergs are
638 generally smaller because they are typically sourced from tidewater glacier fronts rather than calved from
639 larger ice shelves. Arctic icebergs are also logistically easier to observe and access compared to Antarctic
640 icebergs~~Arctic icebergs are generally smaller due to the prevalence of tidewater glacier derived ice rather~~
641 ~~than large ice shelves. Furthermore, due to the much easier logistical situation for observers in the Arctic,~~
642 ~~Arctic icebergs are more easily observed in coastal environments than Antarctic icebergs. Ice observed at~~
643 ~~a distance often appears cleaner than is the case upon closer inspection where sediment layers can be~~
644 ~~better identified. Nevertheless, A~~ comparison of smaller ice fragments from Kongsfjorden in Svalbard
645 and three localities in the Antarctic Peninsula showed that the former had higher sediment loads. Mean
646 sediment loads of 21 g L⁻¹ (median 0.58 g L⁻¹) were previously reported for Kongsfjorden (Hopwood et
647 al., 2019). Average sediment load values for ice fragments handled similarly from the Antarctic
648 Peninsula were 8.5 mg L⁻¹ (median) and mean 430.5 mg L⁻¹ (mean), respectively, which are considerably
649 lower. Contrasting warm/cold-based glaciers and the higher exposed land/ice cover ratio of the coastal
650 glaciated Arctic may explain much of this difference.

651

652 Sediment-rich layers within icebergs have long been hypothesized to be particularly important for the
653 delivery of the micronutrient Fe into the ocean (Hart, 1934) and this has been explicitly confirmed with
654 measurements of dFe and particulate Fe (Lin et al., 2011; Raiswell, 2011). We verify herein, that sediment
655 distribution is a major factor explaining TdFe and TdMn distribution, yet suggest this is a less important
656 factor in explaining dFe, dMn and dSi distribution in icebergs (Fig. 65). The dynamics of sediment-rich
657 layers and their fate in the marine environment is of special interest for trace metal biogeochemistry given
658 the (co)-limiting role these micronutrients have for phytoplankton growth in the Southern Ocean (Hawco
659 et al., 2022; Martin et al., 1990b). Yet multiple factors are likely important for determining the delivery
660 of dFe and dMn to the marine environment because these fluxes do not simply scale with sediment input
661 as per TdFe and TdMn. A close association of TdFe and TdMn is perhaps unsurprising and corroborates
662 a lithogenic origin for the vast majority of Fe present in icebergs. It also suggests limited biogeochemical
663 processing of englacial material and/or rapid loss of basal ice layers preventing the modification of a
664 lithogenic ratio in-between sediment acquisition by icebergs and sediment release in the ocean (Forsch et
665 al., 2021).

666

667 ~~A curious observation herein was that cryoconite formation was observed on ice fragments suggesting~~
668 ~~that, as is the case on glacier surfaces (Cook et al., 2015; Rozwalak et al., 2022), this can be an important~~
669 ~~process affecting sediment dynamics on icebergs. The unstable nature of icebergs, especially smaller~~
670 ~~icebergs, means that cryoconite holes are likely to be shorter lived than their glacier counterparts, but they~~
671 ~~still may constitute an important feature via which iceberg embedded sediment is processed. The~~
672 ~~accumulation of sediment as cryoconite could for example impede photochemical processing of particles,~~
673 ~~but also potentially create micro-gradients in O₂, pH and temperature that result in different chemical~~
674 ~~conditions than if particles were homogenously distributed (Rozwalak et al., 2022). On larger, more stable~~
675 ~~tabular icebergs, cryoconite may facilitate the growth of attached diatoms (Ferrario et al., 2012; Robison~~
676 ~~et al., 2011). These processes are well described on glacier surfaces but a critical difference in interpreting~~
677 ~~their significance in iceberg environments is that iceberg movement and rolling is likely to prevent the~~
678 ~~long term development of cryoconite on anything other than large tabular icebergs. Nevertheless, the~~

~~observation of such holes at centimetre size in environments where icebergs are free floating and rapidly disintegrating suggests that they might constitute an underappreciated mechanism of iceberg melt and sediment processing.~~

A further, to our knowledge, novel observation was the tendency of embedded sediment to be rapidly discharged from ice fragments. When collecting larger pieces of ice it was found that, in all cases, embedded sediment was rapidly washed out of the ice fragments largely within the melting of the first 10-20% of ice volume (Supp. Fig. 1). These ice fragments were specifically targeted to avoid ice with surface sediment layers and so this result cannot be explained by the loss of sediment frozen on the surface of ice. If this process was occurring at larger scales in nature it could further act to skew the deposition of iceberg-borne particles towards inshore environments i.e., it would compound the inefficiencies in the delivery of sediment and associated nutrients to the offshore marine environment due to the rapid loss of basal ice layers. The mechanism of this process is unclear, ~~but it is not associated with ongoing cryoconite formation or similar associated processes due to albedo effects because the ice was stored in the dark.~~

4.3 (Micro)nutrient fluxes to the ocean from icebergs

By combining measured concentrations herein with estimates of the ice volume discharged from Greenland and Antarctica, annual flux estimates can be estimated for (micro)nutrients associated with icebergs (Table 1). For the macronutrients NO_3^- , PO_4^{3-} , and dSi, the uncertainty in these flux estimates remains large relative to the magnitude of the flux. This is an inherent result of the large fraction of ice with macronutrient concentrations close to the LOD, so would not be changed with further data collection. Iceberg-derived macronutrient fluxes are likely minor in terms of annual polar pelagic nutrient cycling (Table 1) and in most coastal environments will dilute, rather than enhance, ambient macronutrient concentrations. This is especially the case in Antarctic waters, where macronutrient concentrations are universally high (Boyer et al., 2018). The low macronutrient of ice also implies that physical effects associated with iceberg passage, mixing and any stratification resulting from meltwater are likely larger effects on annual macronutrient budgets for biota than the direct contribution of meltwater (Helly et al.,

2011; Tarling et al., 2024). In regions where meltwater from icebergs accumulates in a thin surface layer, which is a phenomenon largely confined to Arctic fjords (e.g. Enderlin et al., 2016), low macronutrient concentrations may contribute to low primary production in near-surface layers. Although it should be noted that meltwater delivery is not confined to the surface (Moon et al., 2018) and, as noted, can drive the vertical entrainment of macronutrients within the water column.

Nutrient	Greenland Ice Sheet annual discharge Mmol yr⁻¹	Antarctic Ice Sheet annual discharge Mmol yr⁻¹
NO ₃ ⁻	389 ± 345 (370)	418 ± 796 (168)
PO ₄ ³⁻	18 ± 25 (14)	76 ± 83 (58)
dSi	212 ± 701 (27)	476 ± 2187 (b/d)
dFe	7.1 ± 15 (3.9)	130 ± 472 (18)
dMn	2.3 ± 6.0 (0.77)	32 ± 191 (3.3)

Table 1. Annual fluxes of nutrients associated with icebergs assuming calved ice volumes of 500 km³ yr⁻¹ from Greenland and 1100 km³ yr⁻¹ from Antarctica (Bamber et al., 2018; Rignot et al., 2013). Values are mean ± standard deviation (median); ‘b/d’ represents a median sample below detection.

Delivery of total dissolvable Fe and Mn fluxes from icebergs to the ocean may be considerable (Table 1), but, as these components are associated with heterogeneous particle-rich layers in ice, their delivery may be skewed towards inshore waters where primary production is less limited by trace metal availability. Dissolved Fe and Mn components are of more direct relevance to phytoplankton demands on the short-term timescales associated with iceberg passage, due to the short residence time of particle associated metal phases in the marine environment. Annual dFe and dMn fluxes also carry relatively large uncertainties (Table 1) which reflects the wide range of concentrations present in ice. Although the crustal abundance of Mn oxides is approximately 50× lower than that of Fe oxides (Rudnick and Gao, 2004),

728 dMn fluxes from Greenland and Antarctica are 32% and 25% of the corresponding dFe fluxes,
729 respectively (Table 1). Similar trends are evident in dFe and dMn concentrations within fjord
730 environments where trace metals from subglacial discharge and runoff enter the ocean (Forsch et al.,
731 2021; van Genuchten et al., 2022). The relatively-high concentrations of dMn compared to dFe likely
732 reflect the rapid scavenging of dFe close to source compared to more conservative behaviour of dMn over
733 short (hours to days) timescales (Kandel and Aguilar-Islas, 2021; Yang et al., 2022; Zhang et al., 2015).

734
735 A key finding throughout was that the macronutrient and micronutrient content of ice was relatively
736 similar between catchments and regions worldwide despite the contrasting geographic context of Arctic
737 and Antarctic ice calving fronts and notable differences in sediment loads between regions (Fig. 2). There
738 was limited evidence of differences in ice nutrient concentrations between field campaigns returning to
739 the same location (Nuup Kangerlua, southwest Greenland) in different seasons/years and similarly limited
740 evidence of differences contrasting ice fragments collected offshore in Disko Bay (west Greenland), with
741 ice fragments collected inshore close to marine-terminating glacier fronts (Fig. 5). Icebergs are inherently
742 heterogeneous due to the nature of englacial and basal sediment incorporation and loss processes. This
743 heterogeneity combined with generally low nutrient concentrations, appears to mask any regional or
744 catchment specific trends in macronutrient or micronutrient content related to changing bedrock
745 composition (e.g. Halbach et al., 2019), calving dynamics (Smith et al., 2019), or photochemical processes
746 (e.g. Kim et al., 2010).

747
748 Whilst further sampling would not reduce uncertainty in the estimated nutrient fluxes (Table 1), some
749 specific caveats with our present work could be resolved in the future. Herein we have considered only
750 NO_x^- and PO_4^{3-} as sources ~~source~~ of bioaccessible nitrogen and phosphorous, but considering the
751 universally low concentrations present in icebergs, other N and P sources (e.g. DON- Dissolved Organic
752 Nitrogen, DOP- Dissolved Organic Phosphorous, and NH_4) may be relatively important (Parker et al.
753 1978). We hypothesized that a basal ice influence would be present in some ice fragments with high dSi
754 alongside dFe and dMn, but conversely found very low dSi concentrations across all field locations.
755 Future process studies might elucidate the mechanistic reasons why elevated dSi concentrations are not

756 present alongside dFe and dMn concentrations in ice melt. Finally, sediment rich layers of large ice
757 samples were observed to rapidly melt, potentially indicating that these layers are prone to disintegration.
758 Such a mechanism could be an important regulator of sediment dispersion in the marine environment,
759 potentially further skewing the delivery of iceberg rafted debris and nutrients towards coastal waters.
760

761 **5 Conclusions**

762 The dataset reported here covers ice fragments collected from a range of Arctic and Antarctic, polar and
763 (sub)polar marine-terminating glaciers, and floating ice tongues. Throughout, icebergs are found to be
764 only a minor source of macronutrients to the ocean with a large fraction of measurements close to, or
765 below the standard analytical detection limit- especially for PO_4^{3-} and dSi. Icebergs do however deliver
766 modest fluxes of dissolved Fe and Mn to the polar oceans, which are likely important ecologically-
767 particularly in the Southern Ocean (Sedwick et al., 2000; Wu et al., 2019). The rapid dilution of meltwater
768 close to icebergs, typically to concentrations <1% (Helly et al., 2011; Stephenson et al., 2011), means
769 these trace metal inputs are challenging to constrain from in-situ pelagic observations (Lin et al., 2011),
770 thus our measurements provide a first order constraint on iceberg-derived micronutrient fluxes into polar
771 seas. The scavenged-type behaviour of dFe may explain why the dFe:dMn ratio in ice melt is considerably
772 higher than expected from crustal abundances of Fe and Mn oxides, yet this also raises questions about
773 how micronutrients sourced from icebergs behave immediately after release into the ocean. Dissolved Fe
774 may be scavenged close to source limiting the spatial extent of Fe-fertilization from iceberg tracks,
775 whereas, especially in the photic zone, dMn is more stable in seawater (Sunda et al., 1983). Thus icebergs
776 may be an even more disproportionately important dMn source to biota than the dFe:dMn ratio in
777 meltwater suggests.
778

779 **6 Data availability**

780 New data presented herein is available from SeaDataNet [
781 <https://emodnet.ec.europa.eu/geonetwork/emodnet/api/records/ff3c625c-6a39-46ef-b329->

782 222040f85917, last accessed 20/08/2024]. Literature data was compiled from prior published values (De
783 Baar et al., 1995; Campbell and Yeats, 1982; Forsch et al., 2021; Höfer et al., 2019; Hopwood et al., 2017,
784 2019; Lin et al., 2011; Loscher et al., 1997; Martin et al., 1990b). For convenience, a merged dataset is
785 appended for data not previously compiled.

786 **7 Author contribution**

787 MH, DC, JH and EPA designed the study and acquired funding and resources. JK, DC, JD, JH, EA, TL,
788 LM and MH conducted field work. EA, KZ and MH conducted laboratory analysis. JK, JH and MH
789 conducted data analysis. JK and MH wrote the initial draft of the paper and all authors contributed to
790 revision of the text.

791 **8 Competing interests**

792 The authors declare that they have no conflict of interest.

793 **9 Acknowledgements**

794 Tim Steffens (GEOMAR) is thanked for technical assistance with ICP-MS, André Mutzberg (GEOMAR)
795 for macronutrient data, Stephan Krisch (formerly GEOMAR), Thomas Juul-Pedersen (GINR) and Case
796 van Genuchten (GEUS) for assistance with sampling. The captain and crew of RV Sanna are thanked for
797 field support. Antarctic sampling was possible through FONDAP-IDEAL 15150003 and FONDECYT-
798 Regular 1211338 (awarded to JH). MH received support from the DFG (HO 6321/1-1), the GLACE
799 project organised by the Swiss Polar Institute and supported by the Swiss Polar Foundation, NSFC project
800 42150610482 and the European Union H2020 research and innovation programme under grant agreement
801 n° 824077. LM was funded by research programme VENI with project number 016.Veni.192.150
802 financed by the Dutch Research Council (NWO). JD was sponsored by a scholarship from the Instituto
803 Antártico Chileno (INACH), Correos de Chile, and the Fuerza Aérea de Chile (FACH). Ship time and
804 work in Nuup Kangerlua was conducted in collaboration with MarineBasis-Nuuk, part of the Greenland
805 Ecosystem Monitoring project (GEM). We gratefully acknowledge logistics and funding contributions

806 from the Danish Centre for Marine Research (DCH), Greenland Institute of Natural Resources, Novo
807 Nordic Foundation (NNF17SH0028142) and INACH.

808 **10 References**

809 Ackley, S. F. and Sullivan, C. W.: Physical controls on the development and characteristics of Antarctic sea ice biological
810 communities— a review and synthesis, *Deep Sea Research Part I: Oceanographic Research Papers*, 41, 1583–1604,
811 [https://doi.org/10.1016/0967-0637\(94\)90062-0](https://doi.org/10.1016/0967-0637(94)90062-0), 1994.

812
813 Akers, P. D., Savarino, J., Cailion, N., Servettaz, A. P. M., Le Meur, E., Magand, O., Martins, J., Agosta, C., Crockford, P.,
814 Kobayashi, K., Hattori, S., Curran, M., van Ommen, T., Jong, L., & Roberts, J. L. (2022). Sunlight-driven nitrate loss records
815 Antarctic surface mass balance. *Nature Communications*, 13(1), 4274. <https://doi.org/10.1038/s41467-022-31855-7>

816
817 Alley, R. B., Cuffey, K. M., Evenson, E. B., Strasser, J. C., Lawson, D. E., and Larson, G. J.: How glaciers entrain and transport
818 basal sediment: Physical constraints, *Quat Sci Rev*, 16, 1017–1038, [https://doi.org/10.1016/S0277-3791\(97\)00034-6](https://doi.org/10.1016/S0277-3791(97)00034-6), 1997.

819
820 Anderson, J. B., Domack, E. W., and Kurtz, D. D.: Observations of Sediment-laden Icebergs in Antarctic Waters: Implications
821 to Glacial Erosion and Transport, *Journal of Glaciology*, 25, 387–396, <https://doi.org/10.3189/S0022143000015240>, 1980.

822
823 De Baar, H. J. W., De Jong, J. T. M., Bakker, D. C. E., Loscher, B. M., Veth, C., Bathmann, U., and Smetacek, V.: Importance
824 of iron for plankton blooms and carbon dioxide drawdown in the Southern Ocean, *Nature*, 373, 412–415,
825 <https://doi.org/10.1038/373412a0>, 1995.

826
827 Bamber, J. L., Tedstone, A. J., King, M. D., Howat, I. M., Enderlin, E. M., van den Broeke, M. R., and Noel, B.: Land Ice
828 Freshwater Budget of the Arctic and North Atlantic Oceans: 1. Data, Methods, and Results, *J Geophys Res Oceans*, 123, 1827–
829 1837, <https://doi.org/10.1002/2017JC013605>, 2018.

830
831 Boyd, P. W., Arrigo, K. R., Strzepek, R., and Van Dijken, G. L.: Mapping phytoplankton iron utilization: Insights into Southern
832 Ocean supply mechanisms, *J Geophys Res Oceans*, 117, <https://doi.org/10.1029/2011JC007726>, 2012.

833
834 Boyer, T. P., Garcia, H. E., Locarnini, R. A., Zweng, M. M., Mishonov, A. V., Reagan, J. R., Weathers, K. A., Baranova, O.
835 K., Seidov, D., and Smolyar, I. V.: *World Ocean Atlas 2018*, 2018.

836

837 Browning, T. J., Achterberg, E. P., Engel, A., and Mawji, E.: Manganese co-limitation of phytoplankton growth and major
838 nutrient drawdown in the Southern Ocean, *Nat Commun*, 12, 884, <https://doi.org/10.1038/s41467-021-21122-6>, 2021.

839

840 Campbell, J. A. and Yeats, P. A.: The distribution of manganese, iron, nickel, copper and cadmium in the waters of Baffin Bay
841 and the Canadian Arctic Archipelago, *Oceanologica Acta*, 5, <https://doi.org/10.1007/s00128-002-0077-7>, 1982.

842

843 ~~Cantoni, C., Hopwood, M. J., Clarke, J. S., Chiggiato, J., Achterberg, E. P., and Cozzi, S.: Glacial drivers of marine
844 biogeochemistry indicate a future shift to more corrosive conditions in an Arctic fjord, *J Geophys Res Biogeosci*, 125,
845 e2020JG005633, <https://doi.org/10.1029/2020JG005633>, 2020.~~

846

847 Cook, J., Edwards, A., Takeuchi, N., and Irvine-Fynn, T.: Cryoconite: The dark biological secret of the cryosphere, *Progress
848 in Physical Geography: Earth and Environment*, 40, 66–111, <https://doi.org/10.1177/0309133315616574>, 2015.

849

850 Craven, M., Allison, I., Fricker, H. A., and Warner, R.: Properties of a marine ice layer under the Amery Ice Shelf, East
851 Antarctica, *Journal of Glaciology*, 55, 717–728, <https://doi.org/10.3189/002214309789470941>, 2009.

852

853 Dowdeswell, J. A. and Dowdeswell, E. K.: Debris in Icebergs and Rates of Glaci-Marine Sedimentation: Observations from
854 Spitsbergen and a Simple Model, *J Geol*, 97, 221–231, <https://doi.org/10.1086/629296>, 1989.

855

856 Enderlin, E. M., Hamilton, G. S., Straneo, F., and Sutherland, D. A.: Iceberg meltwater fluxes dominate the freshwater budget
857 in Greenland’s iceberg-congested glacial fjords, *Geophys Res Lett*, 43, <https://doi.org/10.1002/2016GL070718>, 2016.

858

859 ~~Ferrario, M. E., Cefarelli, A. O., Robison, B., and Vernet, M.: *Thalassioneis signyensis* (bacillariophyceae) from northwest
860 Weddell Sea icebergs, an emendation of the generic description, *J Phycol*, 48, 222–230, <https://doi.org/10.1111/j.1529-8817.2011.01097.x>, 2012.~~

861

862

863 Fischer, H., Wagenbach, D., and Kipfstuhl, J.: Sulfate and nitrate firn concentrations on the Greenland ice sheet: 1. Large-
864 scale geographical deposition changes, *Journal of Geophysical Research: Atmospheres*, 103, 21927–21934,
865 <https://doi.org/10.1029/98JD01885>, 1998.

866

867 Fischer, H., Schüpbach, S., Gfeller, G., Bigler, M., Röthlisberger, R., Erhardt, T., Stocker, T. F., Mulvaney, R., and Wolff, E.
868 W.: Millennial changes in North American wildfire and soil activity over the last glacial cycle, *Nat Geosci*, 8, 723–727,
869 <https://doi.org/10.1038/ngeo2495>, 2015.

870

871 Forsch, K. O., Hahn-Woernle, L., Sherrell, R. M., Rocanova, V. J., Bu, K., Burdige, D., Vernet, M., and Barbeau, K. A.:
872 Seasonal dispersal of fjord meltwaters as an important source of iron and manganese to coastal Antarctic phytoplankton,
873 *Biogeosciences*, 18, 6349–6375, <https://doi.org/10.5194/bg-18-6349-2021>, 2021.
874

875 van Genuchten, C. M., Hopwood, M. J., Liu, T., Krause, J., Achterberg, E. P., Rosing, M. T., and Meire, L.: Solid-phase Mn
876 speciation in suspended particles along meltwater-influenced fjords of West Greenland, *Geochim Cosmochim Acta*, 326, 180–
877 198, <https://doi.org/10.1016/j.gca.2022.04.003>, 2022.
878

879 Gleitz, M., v.d. Loeff, M. R., Thomas, D. N., Dieckmann, G. S., and Millero, F. J.: Comparison of summer and winter inorganic
880 carbon, oxygen and nutrient concentrations in Antarctic sea ice brine, *Mar Chem*, 51, 81–91, [https://doi.org/10.1016/0304-](https://doi.org/10.1016/0304-4203(95)00053-T)
881 [4203\(95\)00053-T](https://doi.org/10.1016/0304-4203(95)00053-T), 1995.
882

883 Grotti, M., Soggia, F., Ianni, C., and Frache, R.: Trace metals distributions in coastal sea ice of Terra Nova Bay, Ross Sea,
884 *Antarctica, Antarct Sci*, 17, 289–300, <https://doi.org/10.1017/S0954102005002695>, 2005.
885

886 Günther, S. and Dieckmann, G. S.: Seasonal development of algal biomass in snow-covered fast ice and the underlying platelet
887 layer in the Weddell Sea, *Antarctica, Antarct Sci*, 11, 305–315, <https://doi.org/10.1017/S0954102099000395>, 1999.
888

889 Gutt, J., Starmans, A., and Dieckmann, G.: Impact of iceberg scouring on polar benthic habitats, *Mar Ecol Prog Ser*, 137, 311–
890 316, <https://doi.org/10.3354/meps137311>, 1996.
891

892 Halbach, L., Vihtakari, M., Duarte, P., Everett, A., Granskog, M. A., Hop, H., Kauko, H. M., Kristiansen, S., Myhre, P. I.,
893 Pavlov, A. K., Pramanik, A., Tatarek, A., Torsvik, T., Wiktor, J. M., Wold, A., Wulff, A., Steen, H., and Assmy, P.: Tidewater
894 Glaciers and Bedrock Characteristics Control the Phytoplankton Growth Environment in a Fjord in the Arctic,
895 <https://doi.org/10.3389/fmars.2019.00254>, 2019.
896

897 Hansen, H. P. and Koroleff, F.: Determination of nutrients, in: *Methods of seawater analysis*, edited by: Grasshoff, K., K.
898 Kremling, and Ehrhardt, M., Wiley-VCH Verlag GmbH, 159–228, 1999.
899

900 Hansson, M. E.: The Renland ice core. A Northern Hemisphere record of aerosol composition over 120,000 years, *Tellus B:*
901 *Chemical and Physical Meteorology*, 46, 390–418, 1994.
902

903 Hart, T. J.: *Discovery Reports*, *Discovery Reports*, VIII, 1–268, 1934.
904

905 Hawco, N. J., Tagliabue, A., and Twining, B. S.: Manganese Limitation of Phytoplankton Physiology and Productivity in the
906 Southern Ocean, *Global Biogeochem Cycles*, 36, e2022GB007382, <https://doi.org/10.1029/2022GB007382>, 2022.

907

908 Hawkings, J. R., Wadham, J. L., Benning, L. G., Hendry, K. R., Tranter, M., Tedstone, A., Nienow, P., and Raiswell, R.: Ice
909 sheets as a missing source of silica to the polar oceans, 8, 14198, 2017.

910

911 Hawkings, J. R., Skidmore, M. L., Wadham, J. L., Priscu, J. C., Morton, P. L., Hatton, J. E., Gardner, C. B., Kohler, T. J.,
912 Stibal, M., Bagshaw, E. A., Steigmeyer, A., Barker, J., Dore, J. E., Lyons, W. B., Tranter, M., and Spencer, R. G. M.: Enhanced
913 trace element mobilization by Earth's ice sheets, *Proceedings of the National Academy of Sciences*, 117, 31648–31659,
914 <https://doi.org/10.1073/pnas.2014378117>, 2020.

915

916 Helly, J. J., Kaufmann, R. S., Stephenson Jr., G. R., and Vernet, M.: Cooling, dilution and mixing of ocean water by free-
917 drifting icebergs in the Weddell Sea, *Deep-Sea Research Part II-Topical Studies in Oceanography*, 58, 1346–1363,
918 <https://doi.org/10.1016/j.dsr2.2010.11.010>, 2011.

919

920 Henley, S. F., Cozzi, S., Fripiat, F., Lannuzel, D., Nomura, D., Thomas, D. N., Meiners, K. M., Vancoppenolle, M., Arrigo,
921 K., Stefels, J., van Leeuwe, M., Moreau, S., Jones, E. M., Fransson, A., Chierici, M., and Delille, B.: Macronutrient
922 biogeochemistry in Antarctic land-fast sea ice: Insights from a circumpolar data compilation, *Mar Chem*, 104324,
923 <https://doi.org/10.1016/j.marchem.2023.104324>, 2023.

924

925 Herraiz-Borreguero, L., Lannuzel, D., van der Merwe, P., Treverrow, A., and Pedro, J. B.: Large flux of iron from the Amery
926 Ice Shelf marine ice to Prydz Bay, East Antarctica, *J Geophys Res Oceans*, 121, 6009–6020,
927 <https://doi.org/10.1002/2016JC011687>, 2016.

928

929 Höfer, J., González, H., Laudien, J., Schmidt, G., Häussermann, V., and Richter, C.: All you can eat: the functional response
930 of the cold-water coral *Desmophyllum dianthus* feeding on krill and copepods, *PeerJ*, 6, <https://doi.org/10.7717/peerj.5872>,
931 2018.

932

933 Höfer, J., Giesecke, R., Hopwood, M. J. M. J., Carrera, V., Alarcón, E., and González, H. E. H. E.: The role of water column
934 stability and wind mixing in the production/export dynamics of two bays in the Western Antarctic Peninsula, *Prog Oceanogr*,
935 174, 105–116, <https://doi.org/10.1016/j.pocean.2019.01.005>, 2019.

937 [Hopwood, M. J., Connelly, D. P., Arendt, K. E., Juul-Pedersen, T., Stinchcombe, M. C., Meire, L., Esposito, M., and Krishna-](#)
938 [R.: Seasonal changes in Fe along a glaciated Greenlandic fjord, *Front Earth Sci \(Lausanne\)*, 4,](#)
939 <https://doi.org/10.3389/feart.2016.00015>, 2016.

940

941 Hopwood, M. J., Cantoni, C., Clarke, J. S., Cozzi, S., and Achterberg, E. P.: The heterogeneous nature of Fe delivery from
942 melting icebergs, *Geochem Perspect Lett*, 3, 200–209, <https://doi.org/10.7185/geochemlet.1723>, 2017.

943

944 Hopwood, M. J., Carroll, D., Höfer, J., Achterberg, E. P., Meire, L., Le Moigne, F. A. C., Bach, L. T., Eich, C., Sutherland,
945 D. A., and González, H. E.: Highly variable iron content modulates iceberg-ocean fertilisation and potential carbon export,
946 *Nat Commun*, 10, 5261, <https://doi.org/10.1038/s41467-019-13231-0>, 2019.

947

948 Huhn, O., Rhein, M., Kanzow, T., Schaffer, J., and Sültenfuß, J.: Submarine Meltwater From Nioghalvfjærdsbræ (79 North
949 Glacier), Northeast Greenland, *J Geophys Res Oceans*, 126, e2021JC017224, <https://doi.org/10.1029/2021JC017224>, 2021.

950

951 [IPCC, 2019: IPCC Special Report on the Ocean and Cryosphere in a Changing Climate \[H.-O. Pörtner, D.C. Roberts, V.](#)
952 [Masson-Delmotte, P. Zhai, M. Tignor, E. Poloczanska, K. Mintenbeck, A. Alegría, M. Nicolai, A. Okem, J. Petzold, B. Rama,](#)
953 [N.M. Weyer \(eds.\)\]. Cambridge University Press, Cambridge, UK and New York, NY, USA, 755 pp.](#)
954 <https://doi.org/10.1017/9781009157964>.

955

956 Kandel, A. and Aguilar-Islas, A.: Spatial and temporal variability of dissolved aluminum and manganese in surface waters of
957 the northern Gulf of Alaska, *Deep Sea Research Part II: Topical Studies in Oceanography*, 104952,
958 <https://doi.org/10.1016/j.dsr2.2021.104952>, 2021.

959

960 Kim, J., Park, Y. K., Koo, T., Jung, J., Kang, I., Kim, K., Park, H., Yoo, K.-C., Rosenheim, B. E., & Conway, T. M. (2024).
961 Microbially-mediated reductive dissolution of Fe-bearing minerals during freeze-thaw cycles. *Geochimica et Cosmochimica*
962 *Acta*, 376, 134–143. <https://doi.org/10.1016/j.gca.2024.05.015>

963

964 Kim, K., Choi, W., Hoffmann, M. R., Yoon, H.-I., and Park, B.-K.: Photoreductive Dissolution of Iron Oxides Trapped in Ice
965 and Its Environmental Implications, *Environ Sci Technol*, 44, 4142–4148, <https://doi.org/10.1021/es9037808>, 2010.

966

967 Kjør, H. A., Dallmayr, R., Gabrieli, J., Goto-Azuma, K., Hirabayashi, M., Svensson, A., and Vallelonga, P.: Greenland ice
968 cores constrain glacial atmospheric fluxes of phosphorus, *Journal of Geophysical Research: Atmospheres*, 120, 10, 810, 822,
969 <https://doi.org/10.1002/2015JD023559>, 2015.

970

Formatted: Default Paragraph Font

971 Knight, P. G.: The basal ice layer of glaciers and ice sheets, *Quat Sci Rev*, 16, 975–993, <https://doi.org/10.1016/S0277->
972 [3791\(97\)00033-4](https://doi.org/10.1016/S0277-3791(97)00033-4), 1997.

973

974 Krause, J., Hopwood, M. J., Höfer, J., Krisch, S., Achterberg, E. P., Alarcón, E., Carroll, D., González, H. E., Juul-Pedersen,
975 T., Liu, T., Lodeiro, P., Meire, L., and Rosing, M. T.: Trace Element (Fe, Co, Ni and Cu) Dynamics Across the Salinity
976 Gradient in Arctic and Antarctic Glacier Fjords, *Front Earth Sci (Lausanne)*, 9, 878, <https://doi.org/10.3389/feart.2021.725279>,
977 2021.

978

979 Krause, J. W., Duarte, C. M., Marquez, I. A., Assmy, P., Fernández-Méndez, M., Wiedmann, I., Wassmann, P., Kristiansen,
980 S., and Agustí, S.: Biogenic silica production and diatom dynamics in the Svalbard region during spring, *Biogeosciences*, 15,
981 6503–6517, <https://doi.org/10.5194/bg-15-6503-2018>, 2018.

982

983 Krause, J. W., Schulz, I. K., Rowe, K. A., Dobbins, W., Winding, M. H. S., Sejr, M. K., Duarte, C. M., and Agustí, S.: Silicic
984 acid limitation drives bloom termination and potential carbon sequestration in an Arctic bloom, *Sci Rep*,
985 <https://doi.org/10.1038/s41598-019-44587-4>, 2019.

986

987 Krisch, S., Browning, T. J., Graeve, M., Ludwichowski, K.-U., Lodeiro, P., Hopwood, M. J., Roig, S., Yong, J.-C., Kanzow,
988 T., and Achterberg, E. P.: The influence of Arctic Fe and Atlantic fixed N on summertime primary production in Fram Strait,
989 North Greenland Sea, *Sci Rep*, 10, 15230, <https://doi.org/10.1038/s41598-020-72100-9>, 2020.

990

991 Latour, P., Wuttig, K., van der Merwe, P., Strzepak, R. F., Gault-Ringold, M., Townsend, A. T., Holmes, T. M., Corkill, M.,
992 and Bowie, A. R.: Manganese biogeochemistry in the Southern Ocean, from Tasmania to Antarctica, *Limnol Oceanogr*, 66,
993 2547–2562, <https://doi.org/10.1002/lno.11772>, 2021.

994

995 Laufer-Meiser, K., Michaud, A. B., Maisch, M., Byrne, J. M., Kappler, A., Patterson, M. O., Røy, H., and Jørgensen, B. B.:
996 Potentially bioavailable iron produced through benthic cycling in glaciated Arctic fjords of Svalbard, *Nat Commun*, 12, 1349,
997 <https://doi.org/10.1038/s41467-021-21558-w>, 2021.

998

999 Lewis, E. L. and Perkin, R. G.: Ice pumps and their rates, *J Geophys Res Oceans*, 91, 11756–11762,
1000 <https://doi.org/10.1029/JC091iC10p11756>, 1986.

1001

1002 Lin, H. and Twining, B. S.: Chemical speciation of iron in Antarctic waters surrounding free-drifting icebergs, *Mar Chem*,
1003 128, 81–91, <https://doi.org/10.1016/j.marchem.2011.10.005>, 2012.

1004

1005 Lin, H., Rauschenberg, S., Hexel, C. R., Shaw, T. J., and Twining, B. S.: Free-drifting icebergs as sources of iron to the
1006 Weddell Sea, Deep-Sea Research Part II-Topical Studies in Oceanography, 58, 1392–1406,
1007 <https://doi.org/10.1016/j.dsr2.2010.11.020>, 2011.

1008

1009 Lippiatt, S. M., Lohan, M. C., and Bruland, K. W.: The distribution of reactive iron in northern Gulf of Alaska coastal waters,
1010 Mar Chem, 121, 187–199, <https://doi.org/10.1016/j.marchem.2010.04.007>, 2010.

1011

1012 Loscher, B. M., DeBaar, H. J. W., DeJong, J. T. M., Veth, C., and Dehairs, F.: The distribution of Fe in the Antarctic
1013 Circumpolar Current, Deep-Sea Research Part II-Topical Studies in Oceanography, 44, 143–187,
1014 [https://doi.org/10.1016/S0967-0645\(96\)00101-4](https://doi.org/10.1016/S0967-0645(96)00101-4), 1997.

1015

1016 Martin, J. H.: Glacial-interglacial CO₂ change : The iron hypothesis, Paleoclimatology, 5, 1–13, 1990.

1017

1018 Martin, J. H., Fitzwater, S. E., and Gordon, R. M.: Iron deficiency limits phytoplankton growth in Antarctic waters, Global
1019 Biogeochem Cycles, 4, 5–12, 1990a.

1020

1021 Martin, J. H., Gordon, R. M., and Fitzwater, S. E.: Iron in Antarctic waters, Nature, 345, 156–158,
1022 <https://doi.org/10.1038/345156a0>, 1990b.

1023

1024 Meire, L., Meire, P., Struyf, E., Krawczyk, D. W., Arendt, K. E., Yde, J. C., Juul Pedersen, T., Hopwood, M. J., Rysgaard, S.,
1025 and Meysman, F. J. R.: High export of dissolved silica from the Greenland Ice Sheet, Geophys Res Lett, 43,
1026 <https://doi.org/10.1002/2016GL070191>, 2016.

1027

1028 Meire, L., Mortensen, J., Meire, P., Juul-Pedersen, T., Sejr, M. K., Rysgaard, S., Nygaard, R., Huybrechts, P., and Meysman,
1029 F. J. R.: Marine-terminating glaciers sustain high productivity in Greenland fjords, Glob Chang Biol, 23, 5344–5357,
1030 <https://doi.org/10.1111/gcb.13801>, 2017.

1031

1032 Moon, T., Sutherland, D. A., Carroll, D., Felikson, D., Kehrl, L., & Straneo, F. (2018). Subsurface iceberg melt key to
1033 Greenland fjord freshwater budget. *Nature Geoscience*. <https://doi.org/10.1038/s41561-017-0018-z>

1034

1035 Moore, C. M., Mills, M. M., Arrigo, K. R., Berman-Frank, I., Bopp, L., Boyd, P. W., Galbraith, E. D., Geider, R. J., Guieu,
1036 C., Jaccard, S. L., Jickells, T. D., La Roche, J., Lenton, T. M., Mahowald, N. M., Maranon, E., Marinov, I., Moore, J. K.,
1037 Nakatsuka, T., Oschlies, A., Saito, M. A., Thingstad, T. F., Tsuda, A., and Ulloa, O.: Processes and patterns of oceanic nutrient
1038 limitation, Nature Geosci, 6, 701–710, <https://doi.org/10.1038/ngeo1765>, 2013.

1039
1040 Mugford, R. I., & Dowdeswell, J. A. (2010). Modeling iceberg-rafted sedimentation in high-latitude fjord environments.
1041 *Journal of Geophysical Research: Earth Surface*, 115(3). <https://doi.org/10.1029/2009JF001564>
1042
1043 Nielsdottir, M. C., Moore, C. M., Sanders, R., Hinz, D. J., and Achterberg, E. P.: Iron limitation of the postbloom
1044 phytoplankton communities in the Iceland Basin, *Global Biogeochem Cycles*, 23, <https://doi.org/10.1029/2008gb003410>,
1045 2009.
1046
1047 Neubauer, J., & Heumann, K. G. (1988). Nitrate trace determinations in snow and firn core samples of ice shelves at the
1048 weddell sea, Antarctica. *Atmospheric Environment (1967)*, 22(3), 537–545. [https://doi.org/10.1016/0004-6981\(88\)90197-7](https://doi.org/10.1016/0004-6981(88)90197-7)
1049
1050 Nomura, D., Sahashi, R., Takahashi, K. D., Makabe, R., Ito, M., Tozawa, M., Wongpan, P., Matsuda, R., Sano, M., Yamamoto-
1051 Kawai, M., Nojiri, N., Tachibana, A., Kurosawa, N., Moteki, M., Tamura, T., Aoki, S., and Murase, H.: Biogeochemical
1052 characteristics of brash sea ice and icebergs during summer and autumn in the Indian sector of the Southern Ocean, *Prog*
1053 *Oceanogr.* 214, 103023, <https://doi.org/10.1016/j.pocean.2023.103023>, 2023.
1054
1055 Oerter, H., Kipfstuhl, J., Determann, J., Miller, H., Wagenbach, D., Minikin, A., and Graft, W.: Evidence for basal marine ice
1056 in the Filchner–Ronne ice shelf, *Nature*, 358, 399–401, <https://doi.org/10.1038/358399a0>, 1992.
1057
1058 Oksanen, J., Blanchet, F. G., Friendly, M., Kindt, R., Legendre, P., McGlenn, D., Minchin, P. R., O’Hara, R. B., Simpson, G.
1059 L., Solymos, P., H., M. H., Stevens, Szoecs, E., and Wagner, H.: *vegan: Community Ecology Package*, 2020.
1060
1061 Parker, B. C., Heiskell, L. E., Thompson, W., and Zeller, E. J.: Non-biogenic fixed nitrogen in Antarctica and some ecological
1062 implications, *Nature*, 271, 651–652, <https://doi.org/10.1038/271651a0>, 1978.
1063
1064 Peñuelas, J., Sardans, J., Rivas-ubach, A., and Janssens, I. A.: The human-induced imbalance between C, N and P in Earth’s
1065 life system, *Glob Chang Biol*, 18, 3–6, <https://doi.org/10.1111/j.1365-2486.2011.02568.x>, 2012.
1066
1067 Person, R., Vancoppenolle, M., Aumont, O., and Malsang, M.: Continental and Sea Ice Iron Sources Fertilize the Southern
1068 Ocean in Synergy, *Geophys Res Lett*, n/a, e2021GL094761, <https://doi.org/10.1029/2021GL094761>, 2021.
1069
1070 R Core Team: *R: A Language and Environment for Statistical Computing*, 2023.
1071

1072 Raiswell, R.: Iceberg-hosted nanoparticulate Fe in the Southern Ocean: Mineralogy, origin, dissolution kinetics and source of
1073 bioavailable Fe, *Deep-Sea Research Part II-Topical Studies in Oceanography*, 58, 1364–1375,
1074 <https://doi.org/10.1016/j.dsr2.2010.11.011>, 2011.

1075
1076 Raiswell, R., Benning, L. G., Tranter, M., and Tulaczyk, S.: Bioavailable iron in the Southern Ocean: the significance of the
1077 iceberg conveyor belt, *Geochem Trans*, 9, <https://doi.org/10.1186/1467-4866-9-7>, 2008.

1078
1079 ~~Raiswell, R., Hawkings, J. R., Benning, L. G., Baker, A. R., Death, R., Albani, S., Mahowald, N., Krom, M. D., Poulton, S.~~
1080 ~~W., Wadham, J., and Tranter, M.: Potentially bioavailable iron delivery by iceberg-hosted sediments and atmospheric dust to~~
1081 ~~the polar oceans, *Biogeosciences*, 13, 3887–3900, <https://doi.org/10.5194/bg-13-3887-2016>, 2016.~~

1082
1083 Randelhoff, A., Holding, J., Janout, M., Sejr, M. K., Babin, M., Tremblay, J. É., and Alkire, M. B.: Pan-Arctic Ocean Primary
1084 Production Constrained by Turbulent Nitrate Fluxes, *Front Mar Sci*, <https://doi.org/10.3389/fmars.2020.00150>, 2020.

1085
1086 Redfield, A. C.: On the proportions of organic derivations in sea water and their relation to the composition of plankton, in:
1087 James Johnstone Memorial Volume, edited by: Daniel, R. J., University Press of Liverpool, Liverpool, 177–192, 1934.

1088
1089 Rignot, E., Jacobs, S., Mouginit, J., and Scheuchl, B.: Ice-Shelf Melting Around Antarctica, *Science* (1979), 341, 266–270,
1090 <https://doi.org/10.1126/science.1235798>, 2013.

1091
1092 ~~Robison, B. H., Vernet, M., and Smith, K. L.: Algal communities attached to free drifting, Antarctic icebergs, *Deep Sea*~~
1093 ~~*Research Part II: Topical Studies in Oceanography*, 58, 1451–1456, <https://doi.org/10.1016/j.dsr2.2010.11.024>, 2011.~~

1094
1095 Rozwalak, P., Podkowa, P., Buda, J., Niedzielski, P., Kawecki, S., Ambrosini, R., Azzoni, R. S., Baccolo, G., Ceballos, J. L.,
1096 Cook, J., Di Mauro, B., Ficetola, G. F., Franzetti, A., Ignatiuk, D., Klimaszky, P., Łokas, E., Ono, M., Parnikoza, I., Pietryka,
1097 M., Pittino, F., Poniecka, E., Porazinska, D. L., Richter, D., Schmidt, S. K., Sommers, P., Souza-Kasprzyk, J., Stibal, M.,
1098 Szczuciński, W., Uetake, J., Wejnerowski, Ł., Yde, J. C., Takeuchi, N., and Zawierucha, K.: Cryoconite – From minerals and
1099 organic matter to bioengineered sediments on glacier’s surfaces, *Science of The Total Environment*, 807, 150874,
1100 <https://doi.org/10.1016/j.scitotenv.2021.150874>, 2022.

1101
1102 Rudnick, R. L. and Gao, S.: Composition of the continental crust, in: *Treatise on geochemistry*, vol 3 The Crust, edited by:
1103 Holland, H. D. and Turekian, K. K., Elsevier, Amsterdam, 1–65, 2004.

1105 Ryan-Keogh, T. J., Macey, A. I., Nielsdottir, M. C., Lucas, M. I., Steigenberger, S. S., Stinchcombe, M. C., Achterberg, E. P.,
1106 Bibby, T. S., and Moore, C. M.: Spatial and temporal development of phytoplankton iron stress in relation to bloom dynamics
1107 in the high-latitude North Atlantic Ocean, *Limnol Oceanogr*, 58, 533–545, <https://doi.org/10.4319/lo.2013.58.2.0533>, 2013.
1108

1109 Schwarz, J. N. and Schodlok, M. P.: Impact of drifting icebergs on surface phytoplankton biomass in the Southern Ocean:
1110 Ocean colour remote sensing and in situ iceberg tracking, *Deep Sea Res 1 Oceanogr Res Pap*, 56, 1727–1741,
1111 <https://doi.org/10.1016/j.dsr.2009.05.003>, 2009.
1112

1113 Sedwick, P. N., DiTullio, G. R., and Mackey, D. J.: Iron and manganese in the Ross Sea, Antarctica: Seasonal iron limitation
1114 in Antarctic shelf waters, *Journal of Geophysical Research-Oceans*, 105, 11321–11336, <https://doi.org/10.1029/2000jc000256>,
1115 2000.
1116

1117 Shaw, T. J., Raiswell, R., Hexel, C. R., Vu, H. P., Moore, W. S., Dudgeon, R., and Smith Jr., K. L.: Input, composition, and
1118 potential impact of terrigenous material from free-drifting icebergs in the Weddell Sea, *Deep-Sea Research Part II-Topical
1119 Studies in Oceanography*, 58, 1376–1383, <https://doi.org/10.1016/j.dsr2.2010.11.012>, 2011.
1120

1121 Shulenberg, E. (1983). Water-column studies near a melting Arctic iceberg. *Polar Biology*, 2(3), 149–158.
1122 <https://doi.org/10.1007/BF00448964>
1123

1124 Smith Jr., K. L., Robison, B. H., Helly, J. J., Kaufmann, R. S., Ruhl, H. A., Shaw, T. J., Twining, B. S., and Vernet, M.: Free-
1125 drifting icebergs: Hot spots of chemical and biological enrichment in the Weddell Sea, *Science* (1979), 317, 478–482,
1126 <https://doi.org/10.1126/science.1142834>, 2007.
1127

1128 Smith, J. A., Graham, A. G. C., Post, A. L., Hillenbrand, C.-D., Bart, P. J., and Powell, R. D.: The marine geological imprint
1129 of Antarctic ice shelves, *Nat Commun*, 10, 5635, <https://doi.org/10.1038/s41467-019-13496-5>, 2019.
1130

1131 Stephenson, G. R., Sprintall, J., Gille, S. T., Vernet, M., Helly, J. J., and Kaufmann, R. S.: Subsurface melting of a free-floating
1132 Antarctic iceberg, *Deep Sea Research Part II: Topical Studies in Oceanography*, 58, 1336–1345,
1133 <https://doi.org/10.1016/j.dsr2.2010.11.009>, 2011.
1134

1135 Stibal, M., Box, J. E., Cameron, K. A., Langen, P. L., Yallop, M. L., Mottram, R. H., Khan, A. L., Molotch, N. P., Christmas,
1136 N. A. M., Cali Quaglia, F., Remias, D., Smeets, C. J. P. P., van den Broeke, M. R., Ryan, J. C., Hubbard, A., Tranter, M., van
1137 As, D., and Ahlstrøm, A. P.: Algae Drive Enhanced Darkening of Bare Ice on the Greenland Ice Sheet, *Geophys Res Lett*, 44,
1138 11, 411–463, 471, <https://doi.org/10.1002/2017GL075958>, 2017.

1139

1140 Sunda, W. G. and Huntsman, S. A.: Effect of sunlight on redox cycles of manganese in the southwestern Sargasso Sea, Deep
1141 Sea Research Part A, Oceanographic Research Papers, 35, 1297–1317, [https://doi.org/10.1016/0198-0149\(88\)90084-2](https://doi.org/10.1016/0198-0149(88)90084-2), 1988.

1142

1143 Sunda, W. G., Huntsman, S. a., and Harvey, G. R.: Photoreduction of manganese oxides in seawater and its geochemical and
1144 biological implications, Nature, 301, 234–236, <https://doi.org/10.1038/301234a0>, 1983.

1145

1146 Syvitski, J. P. M., Burrell, D. C., & Skei, J. M. (1987). Fjords. Springer New York. [https://doi.org/10.1007/978-1-4612-4632-](https://doi.org/10.1007/978-1-4612-4632-9)
1147 9

1148

1149 Tarling, G. A., Thorpe, S. E., Henley, S. F., Burson, A., Liszka, C. M., Manno, C., Lucas, N. S., Ward, F., Hendry, K. R.,
1150 Malcolm S. Woodward, E., Wootton, M., and Povl Abrahamsen, E.: Collapse of a giant iceberg in a dynamic Southern Ocean
1151 marine ecosystem: In situ observations of A-68A at South Georgia, Prog Oceanogr, 226, 103297, <https://doi.org/10.1016/j.pocean.2024.103297>, 2024.

1152

1153 ~~Taylor, R. L., Semeniuk, D. M., Payne, C. D., Zhou, J., Tremblay, J. É., Cullen, J. T., and Maldonado, M. T.: Colimitation by
1154 light, nitrate, and iron in the Beaufort Sea in late summer, J Geophys Res Oceans, 118, 3260–3277,
1155 <https://doi.org/10.1002/jgre.20244>, 2013.~~

1156

1157 Tournadre, J., Bouhier, N., Girard-Arduin, F., and Rémy, F.: Antarctic icebergs distributions 1992–2014, J Geophys Res
1158 Oceans, 121, 327–349, <https://doi.org/10.1002/2015JC011178>, 2016.

1159

1160 Tranter, M., Skidmore, M., and Wadham, J.: Hydrological controls on microbial communities in subglacial environments,
1161 Hydrol Process, 19, 995–998, <https://doi.org/10.1002/hyp.5854>, 2005.

1162

1163 Trefault, N., De la Iglesia, R., Moreno-Pino, M., Lopes dos Santos, A., Gériques Ribeiro, C., Parada-Pozo, G., Cristi, A., Marie,
1164 D., and Vaultot, D.: Annual phytoplankton dynamics in coastal waters from Fildes Bay, Western Antarctic Peninsula, Sci Rep,
1165 11, 1368, <https://doi.org/10.1038/s41598-020-80568-8>, 2021.

1166

1167 Vancoppenolle, M., Goosse, H., de Montety, A., Fichefet, T., Tremblay, B., and Tison, J.-L.: Modeling brine and nutrient
1168 dynamics in Antarctic sea ice: The case of dissolved silica, J Geophys Res Oceans, 115,
1169 <https://doi.org/10.1029/2009JC005369>, 2010.

1170

1171

1172 Vernet, M., Sines, K., Chakos, D., Cefarelli, A. O., and Ekern, L.: Impacts on phytoplankton dynamics by free-drifting icebergs
1173 in the NW Weddell Sea, *Deep Sea Research Part II: Topical Studies in Oceanography*, 58, 1422–1435,
1174 <https://doi.org/10.1016/j.dsr2.2010.11.022>, 2011.

1175

1176 Wadham, J. L., Tranter, M., Skidmore, M., Hodson, A. J., Priscu, J., Lyons, W. B., Sharp, M., Wynn, P., and Jackson, M.:
1177 Biogeochemical weathering under ice: Size matters, *Global Biogeochem Cycles*, 24, <https://doi.org/10.1029/2009gb003688>,
1178 2010.

1179 ~~Wadley, M. R., Jickells, T. D., and Heywood, K. J.: The role of iron sources and transport for Southern Ocean productivity,
1180 *Deep Sea Research Part I Oceanographic Research Papers*, 87, 82–94, <https://doi.org/10.1016/j.dsr.2014.02.003>, 2014.~~

1181

1182

1183 Wehrmann, L. M., Formolo, M. J., Owens, J. D., Raiswell, R., Ferdelman, T. G., Riedinger, N., and Lyons, T. W.: Iron and
1184 manganese speciation and cycling in glacially influenced high-latitude fjord sediments (West Spitsbergen, Svalbard): Evidence
1185 for a benthic recycling-transport mechanism, <https://doi.org/10.1016/j.gca.2014.06.007>, 2013.

1186

1187 Woodworth-Lynas, C. M. T., Josenhans, H. W., Barrie, J. V., Lewis, C. F. M., and Parrott, D. R.: The physical processes of
1188 seabed disturbance during iceberg grounding and scouring, *Cont Shelf Res*, 11, 939–961, [https://doi.org/10.1016/0278-](https://doi.org/10.1016/0278-4343(91)90086-L)
1189 [4343\(91\)90086-L](https://doi.org/10.1016/0278-4343(91)90086-L), 1991.

1190

1191 Wu, M., McCain, J. S. P., Rowland, E., Middag, R., Sandgren, M., Allen, A. E., and Bertrand, E. M.: Manganese and iron
1192 deficiency in Southern Ocean *Phaeocystis antarctica* populations revealed through taxon-specific protein indicators, *Nat*
1193 *Commun*, 10, 3582, <https://doi.org/10.1038/s41467-019-11426-z>, 2019.

1194

1195 Wu, S.-Y. and Hou, S.: Impact of icebergs on net primary productivity in the Southern Ocean, *Cryosphere*, 11, 707–722,
1196 <https://doi.org/10.5194/tc-11-707-2017>, 2017.

1197

1198 Yang, Y., Ren, J., and Zhu, Z.: Distributions and Influencing Factors of Dissolved Manganese in Kongsfjorden and Ny-
1199 Ålesund, Svalbard, *ACS Earth Space Chem*, 6, 1259–1268, <https://doi.org/10.1021/acsearthspacechem.1c00388>, 2022.

1200

1201 Zhang, R., John, S. G., Zhang, J., Ren, J., Wu, Y., Zhu, Z., Liu, S., Zhu, X., Marsay, C. M., and Wenger, F.: Transport and
1202 reaction of iron and iron stable isotopes in glacial meltwaters on Svalbard near Kongsfjorden: From rivers to estuary to ocean,
1203 *Earth Planet Sci Lett*, 424, 201–211, <https://doi.org/10.1016/j.epsl.2015.05.031>, 2015.

1204